

Event-triggered output synchronization of heterogeneous multi-agent systems[†]

J. Almeida^{1,*}, C. Silvestre^{1,2} and A. M. Pascoal¹

¹*Institute for Systems and Robotics (ISR/IST), LARSyS, Instituto Superior Técnico, Universidade de Lisboa, Av. Rovisco Pais 1, 1049-001 Lisboa, Portugal*

²*Department of Electrical and Computer Engineering, Faculty of Science and Technology of the University of Macau, Macau, China*

SUMMARY

This paper proposes a control architecture that employs event-triggered control techniques to achieve output synchronization of a group of heterogeneous linear time-invariant agents. We associate to each agent an event-triggered output regulation controller and an event-triggered reference generator. The event-triggered output regulation controller is designed such that the regulated output of the agent approximately tracks a reference signal provided by the reference generator in the presence of unknown disturbances. The event-triggered reference generator is responsible for synchronizing its internal state across all agents by exchanging information through a communication network linking the agents. We first address the output regulation problem for a single agent where we analyze two event-triggered scenarios. In the first one, the output and input event detectors operate synchronously, meaning that resets are made at the same time instants, while in the second one they operate asynchronously and independently of each other. It is shown that the tracking error is globally bounded for all bounded reference trajectories and all bounded disturbances. We then merge the results on event-triggered output regulation with previous results on event-triggered communication protocols for synchronization of the reference generators to demonstrate that the regulated output of each agent converges to and remains in a neighborhood of the desired reference trajectory and that the closed-loop system does not exhibit Zeno solutions. Several examples are provided to illustrate the advantages and issues of every component of the proposed control architecture.

KEY WORDS: multi-agent systems; sampled-data systems; output regulation; output synchronization; event-triggered control.

1. INTRODUCTION

A survey of applications of multi-agent systems presented in [1] illustrates how local decentralized coordination strategies can be employed so that a desired global behavior is observed. A special class of applications requires the agents to align their states in a well-defined sense, by exchanging information among them through a communication channel. The most well-known problems in this class include consensus (see, e.g., [1–7]), synchronization (see, e.g., [8–11]), and regulation of coupled systems (see, e.g., [12]).

In this paper, we assume that an agent consists of a linear time-invariant (LTI) plant that models its dynamic behavior, a controller that represents the mechanisms that are employed to make the agent behave as desired, and a communication protocol that establishes when information should

[†]This is a pre-print version of the following article:

Almeida, J., Silvestre, C. and Pascoal, A. M. (2016), Event-triggered output synchronization of heterogeneous multi-agent systems. *International Journal of Robust and Nonlinear Control*. doi: 10.1002/rnc.3629, which is available in final form at <http://dx.doi.org/10.1002/rnc.3629>.

*Correspondence to: J. Almeida (e-mail: jalmeida@isr.ist.utl.pt)

be broadcast to other agents. We address the synchronization problem for groups of heterogeneous agents, where by heterogeneous we mean that the plants that model the dynamic behavior of each agent are in general different. The goal is to derive decentralized control laws and communication protocols capable of making desired state variables of each agent converge to the same reference trajectory.

The single agent version of the synchronization problem reduces to a classical problem in control theory known as linear output regulation, which has been thoroughly studied (a comprehensive exposition of this topic may be found in, e.g., [13, 14]). The problem addressed in output regulation consists in finding a feedback controller capable of internally stabilizing a given LTI plant such that its output converges to a desired reference trajectory in the presence of external disturbances. The reference trajectory and the disturbances are modeled as the outputs of systems whose modes (that are known) identify the class of signals under consideration and whose initial conditions (that are arbitrary) represent the degrees of freedom inside this class. In linear output synchronization of multi-agent systems, we are given a set of distinct agents but a common reference model. Even if each agent converges to its own reference trajectory, due to different initial conditions the agents are not guaranteed to follow the same reference trajectory. In order to correct this misalignment, the agents need to communicate with each other.

Due to the digital nature of the control devices and communication network, an additional constraint on the controller design is the fact that local feedback and communications can only occur at discrete time instants. Thus, we employ sampled-data control and coordination laws, by introducing sample and hold devices in key places. The standard approach would be to apply control action and to broadcast information periodically. However, in recent years a different strategy has received attention due to a flurry of theoretical developments. Known as event-triggered control, in this new approach sampling of the output, updates of the control input, and broadcasts of information are only executed when deemed necessary according to some triggering conditions, often dependent on the state trajectory of each agent.

In the single plant case, an event-triggered controller operates as follows. An event detector is responsible for testing if a triggering condition (basically, a function of the state of the plant) is true or false. If true, then a sampling event is triggered. The advantage of this approach versus a periodic sampling strategy is that the control input is only modified when some relevant change of the state of the plant occurs and this typically leads to a reduction of the number of samples required to achieve desired control objectives. For more details regarding event-triggered control, the interested reader is referred to [15–22] for the single plant case and to [23–25] for the case of multiple plants. It is important to point out that in event-triggered control, triggering conditions must be constantly monitored, which may be infeasible for some applications. To circumvent this issue, self-triggered control strategies have been developed where instead of continuously testing a triggering condition, an event scheduler computes when the next event should occur by using information available at the current time instant (see, e.g., [26–30]).

In a multi-agent scenario where agents have to communicate with each other, the event-triggered strategy is even more relevant since the communication medium is often shared by all agents, meaning that if each agent tried to transmit too often, successful communications would become impossible. Hence, by resorting to event-triggered control techniques, a communication protocol that avoids redundant broadcasts of information is sought. Examples of the use of event-triggered control techniques in a multi-agent scenario may be found in [31–33], where event-triggered solutions for the consensus problem are presented.

In this paper, we address the problem of event-triggered output synchronization (note that the consensus problem is a particular type of synchronization problem where the reference trajectory is constant). The control architecture proposed is inspired by and brings together the work reported in [10] for output synchronization of heterogeneous LTI systems in continuous-time, in [34] for output synchronization with event-triggered communications, and in [35] for event-triggered output feedback stabilization of LTI plants. An overview of the proposed control architecture is illustrated in Figure 1. It consists of two components: an event-triggered output regulation controller and an event-triggered reference generator.

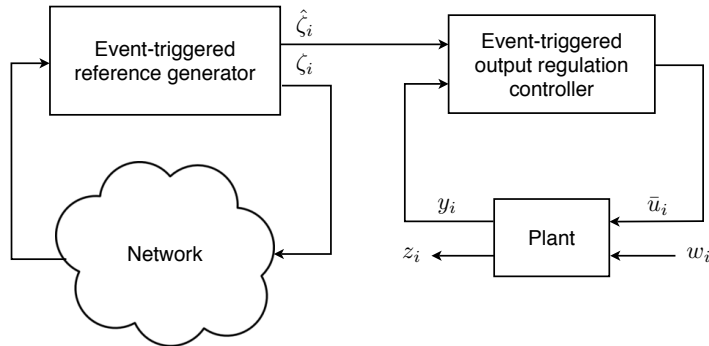


Figure 1. Overview of the proposed control architecture for event-triggered output synchronization from the point of view of agent i .

The event-triggered output regulation controller is responsible for driving the plant through its control input \bar{u}_i such that its regulated output z_i (approximately) follows a desired reference trajectory. The regulation controller has to accomplish this having only access to the measured output of the plant y_i and in the presence of an unknown disturbance w_i . The desired reference trajectory is related with the signal $\hat{\zeta}_i$ provided by the reference generator. The regulation controller is also responsible for deciding when the measured output or the control input of the plant should be sampled or updated, respectively, such that the tracking error remains bounded. The structure of the output regulation controller is based on classical work on output regulation for LTI plants and its event-triggering mechanism is inspired by the work presented in [35].

The event-triggered reference generator has an internal state ζ_i that must evolve in such a way that its trajectory is (approximately) the same across all agents. To accomplish this, the agents need to broadcast to the network from time to time their current internal state and do so according to an event-triggered communication protocol. The structure of the reference generator is borrowed from [10] except that, instead of allowing continuous communication links among agents, here communication is restricted to be discrete in time, which is more suitable for real-world applications. The communication protocol that establishes when a broadcast of the current state of the reference generator should be carried out is borrowed from [32], where it was originally proposed in the context of event-triggered average consensus.

A similar control architecture was considered in preliminary work reported in [33] except that only event-triggered communications were considered (output regulation was still performed in continuous-time). In this paper, we have replaced the continuous-time output regulation controller by an event-triggered output regulation controller, for which we proposed both synchronous and asynchronous solutions for the implementation of the output and input event detectors.

The structure of the output regulation controller used in this paper is based on classical work on output regulation for LTI plants and its event-triggering mechanism is inspired by the work presented in [34] for event-triggered output feedback stabilization of LTI plants. In this paper, we present an event-triggered output regulation controller that extends the results of [34] and that guarantees bounded tracking error for all bounded reference trajectories and exogenous disturbances. Moreover, we use a less conservative technique to derive the event conditions, thereby deriving a triggering mechanism that yields larger average sampling intervals while guaranteeing the same stability conditions.

Related work on event-triggered output regulation is reported in [20] where the authors use an approach that includes both periodic and event-triggered control techniques (this approach is sometimes referred to as periodic event-triggered control; see, e.g., [19]). In this setup, the output of the plant is sampled periodically with a sampling period known in advance and the output event detector is placed between the sampler and the controller. The event detector decides whether or not to transmit the current sampled measurement to the controller based on an event-triggering condition tested at every sampling instant. A similar input event detector is placed between the controller and

the plant. An advantage of this approach is that a minimum time between event times (equal to the sampling period) is guaranteed a priori. Note that in [20], synchronous operation of both the output and input event detection blocks is required (they use the same base sampling period), while in this paper we propose a totally asynchronous solution, where input and output event detectors operate independently of each other.

In summary, the contributions of this paper are twofold:

1. for the single plant case, we present an event-triggered output regulation controller that extends the results of [35] on event-triggered output feedback stabilization and that guarantees bounded tracking error for all bounded reference trajectories and exogenous disturbances;
2. we offer a solution for the event-triggered output synchronization problem for heterogeneous multi-agent systems with fixed network topology that guarantees bounded synchronization errors, obtained by combining the results in the first contribution and the results reported in [34].

The paper is organized as follows. The problem of output synchronization of multi-agent systems is introduced in Section 2, where we review some previous work on the subject and present the architecture of our proposed solution. In Section 3, we address for a single agent the problem of event-triggered output regulation. The proposed output regulation controller is developed and its stability properties are established. Examples are also provided that illustrate several implementation scenarios. In Section 4, we merge the results on output regulation with an event-triggered communication protocol from previous work, to prove that the regulated output of each agent converges to and remains in a neighborhood of the desired reference trajectory and that the closed-loop system does not exhibit Zeno solutions. A multi-agent example is also presented. In Section 5, we summarize the main results. To improve readability, auxiliary material and the proofs of all results have been placed in the Appendix (Section A and Section B, respectively).

Notation The symbols \mathbb{R} , \mathbb{R}_+ , \mathbb{C} , and $\bar{\mathbb{C}}_+$ stand for the sets of real numbers, nonnegative real numbers, complex numbers, and closed right half plane, respectively. If $\{a_k\}_{k \geq 0}$ and $\{b_k\}_{k \geq 0}$ are two strictly increasing sequences with elements in \mathbb{R} , then their union is a sequence $\{c_k\}_{k \geq 0}$ defined as the set of unique elements in $\{a_k\}_{k \geq 0}$ and $\{b_k\}_{k \geq 0}$ reordered to satisfy $c_k < c_{k+1}$ for all $k \geq 0$. We denote this by writing $\{c_k\}_{k \geq 0} = \{a_k\}_{k \geq 0} \cup \{b_k\}_{k \geq 0}$. For $z \in \mathbb{C}$, $\Re\{z\}$ and $\Im\{z\}$ denote its real and imaginary parts, respectively. For a signal $x : \mathbb{R}_+ \rightarrow \mathbb{R}^n$, if the limit from below at time $t \in \mathbb{R}_+$ exists, then it is defined as $x^-(t) = \lim_{s \uparrow t} x(s)$. If t is understood from context, we simply write x and x^- to stand for $x(t)$ and $x^-(t)$, respectively. The notation $\|x\|_{\mathcal{L}_\infty}$ denotes the \mathcal{L}_∞ norm of a signal $x : [t_0, +\infty) \rightarrow \mathbb{R}^n$, defined as $\sup_{t \geq t_0} \|x(t)\|$ where $\|\cdot\|$ stands for the usual Euclidean norm. A vector of dimension n whose entries are all equal to one is denoted by $\mathbf{1}_n$. Given a collection of vectors $\{x_1, \dots, x_N\}$ where $x_i \in \mathbb{R}^{n_i}$, the vector obtained by stacking all x_i column-wise is represented by $z = (x_1, \dots, x_N) = [x_1^\top \ \dots \ x_N^\top]^\top \in \mathbb{R}^m$, with $m = \sum_{i=1}^N n_i$. The symbols I_n and 0_n denote the identity matrix and the zero matrix of dimension $n \times n$, respectively. For a square matrix X , e^X denotes its matrix exponential, $\|X\|$ denotes its spectral norm (defined as its largest singular value), and $\sigma(X)$ denotes its spectrum (the set of eigenvalues of X). A symmetric block matrix M defined as $M = \begin{bmatrix} A & B \\ B^\top & C \end{bmatrix}$ is sometimes represented as $M = \begin{bmatrix} A & B \\ * & C \end{bmatrix}$. If A and B are two matrices, then $\text{diag}(A, B) = \begin{bmatrix} A & 0 \\ 0 & B \end{bmatrix}$. A positive (resp. negative) definite matrix Q is denoted by $Q \succ 0$ (resp. $Q \prec 0$). The symbol \otimes denotes the Kronecker product.

2. OUTPUT SYNCHRONIZATION OF MULTI-AGENT SYSTEMS

The multi-agent system that we consider in this paper is composed of N heterogeneous agents. The dynamic behavior of each agent is modeled as an LTI plant with state vector $x_i^p \in \mathbb{R}^{n_i^p}$ and initial

state $x_i^p(t_0^i)$ that satisfies, for all $t \geq t_0^i$,

$$\dot{x}_i^p(t) = A_i^p x_i^p(t) + B_i^p \bar{u}_i(t) + B_i^w w_i(t) \quad (1a)$$

$$y_i(t) = C_i^p x_i^p(t) + C_i^w w_i(t) \quad (1b)$$

$$z_i(t) = E_i^p x_i^p(t) \quad (1c)$$

where $\bar{u}_i \in \mathbb{R}^{n_i^u}$ is the control input, $w_i \in \mathbb{R}^{n_i^w}$ is an exogenous disturbance, $y_i \in \mathbb{R}^{n_i^y}$ is the measured output, and $z_i \in \mathbb{R}^r$ is the regulated output. Matrices A_i^p , B_i^p , B_i^w , C_i^p , C_i^w , and E_i^p are of appropriate dimensions. Without loss of generality, we take $t_0^i = 0$. We assume that the disturbance w_i is generated by an exogenous system with state $w_i \in \mathbb{R}^{n_i^w}$ that satisfies, for all $t \geq 0$,

$$\dot{w}_i(t) = A_i^w w_i(t), \quad (2)$$

where $w_i(0)$ is an unknown initial state.

The objective is to find conditions that guarantee the existence of a control architecture capable of making the synchronization errors $z_i(t) - z_j(t)$ small in some sense. Namely, the signal $z_i(t)$ of each agent must converge to the same reference trajectory, represented by a reference model with internal state $\zeta_0 \in \mathbb{R}^m$ that satisfies, for all $t \geq 0$,

$$\dot{\zeta}_0 = A_r \zeta_0 \quad (3a)$$

$$z_r = E_r \zeta_0, \quad (3b)$$

where $A_r \in \mathbb{R}^{m \times m}$ and $E_r \in \mathbb{R}^{r \times m}$. The reference signal that the regulated output z_i of each agent should track is represented by z_r . The convergence to the reference trajectory must be distributed in the sense that, since ζ_0 is not made available by one node of the network (there is no reference agent), the reference generators must exchange information among them in order to compensate for different initial conditions. Moreover, each agent is only allowed to exchange information with a subset of other agents as defined by the topology of the communication network that is modeled by a graph \mathcal{G}^\dagger , which is assumed fixed over time. Each agent is represented by a vertex and an edge (j, i) in the communication graph \mathcal{G} means that agent i receives information from agent j .

2.1. Previous work

The problem of output synchronization of multi-agent systems when there exist continuous communication links among agents is addressed in [10]. The authors consider N heterogeneous agents each one with dynamics modeled as in (1) except that no disturbances are considered (that is, $B_i^w = 0$ and $C_i^w = 0$ for all $i \in \{1, \dots, N\}$). In [10], the following assumptions are made:

1. the pair (A_i^p, B_i^p) is stabilizable;
2. the pairs (A_i^p, C_i^p) and (A_i^p, E_i^p) are detectable;
3. there exist $m \in \mathbb{N}$, $m \geq 2$ and matrices $A_r \in \mathbb{R}^{m \times m}$, $E_r \in \mathbb{R}^{r \times m}$, $\Pi_i \in \mathbb{R}^{n_i^p \times m}$, and $\Gamma_i \in \mathbb{R}^{n_i^p \times m}$ for $i \in \{1, \dots, N\}$ such that $\sigma(A_r) \subset \mathbb{C}_+$, the pair (A_r, E_r) is observable, and

$$\Pi_i A_r = A_i^p \Pi_i + B_i^p \Gamma_i \quad (4)$$

$$E_r = E_i^p \Pi_i \quad (5)$$

for all $i \in \{1, \dots, N\}$.

These assumptions guarantee that it is possible to change the dynamics of each agent through feedback such that all agents synchronize to the same reference model represented by the pair (A_r, E_r) .

To achieve synchronization, two control components are associated with each agent, the first of which is the reference generator. The reference generator of agent i has an internal state denoted by

[†]See Section A.1 for a brief review of graph theory.

$\zeta_i \in \mathbb{R}^m$ that satisfies, for all $t \geq 0$,

$$\dot{\zeta}_i = A_r \zeta_i + v_i \quad (6)$$

where v_i is a control input. Note that the reference generator of each agent has a copy of the reference model. In general, the reference generators of different agents will not generate the same trajectory due to different initial conditions $\zeta_i(0) \in \mathbb{R}^m$. To compensate for this initial mismatch, the control input v_i is defined as

$$v_i = \sum_{j=1}^N a_{ij} (\zeta_j - \zeta_i), \quad (7)$$

with a_{ij} denoting the entries of the adjacency matrix associated with the communication graph \mathcal{G} . As we will see, this type of decentralized control law asymptotically synchronizes the reference generators of all agents. For the particular case of $m = 1$ and $A_r = 0$, (6)-(7) represent the classical consensus problem for which it is known that if \mathcal{G} is a rooted graph, then there exists $c \in \mathbb{R}$ such that, for all $i \in \{1, \dots, N\}$, ζ_i tends asymptotically to c (see, e.g., [3, 36]).

The second control component is an output regulation controller composed of a Luenberger state observer whose internal state is represented by $x_i^c \in \mathbb{R}^{n_i^p}$ and whose dynamics are given by

$$\dot{x}_i^c = A_i^p x_i^c + B_i^p u_i + L_i (C_i^p x_i^c - y_i), \quad (8)$$

where $L_i \in \mathbb{R}^{n_i^p \times n_i^y}$ is a gain matrix to be designed, and a control law defined as

$$u_i = K_i^p (x_i^c - \Pi_i \zeta_i) + \Gamma_i \zeta_i = K_i^p x_i^c + K_i^r \zeta_i, \quad (9)$$

where $K_i^p \in \mathbb{R}^{n_i^y \times n_i^p}$ is a matrix gain to be designed and $K_i^r = \Gamma_i - K_i^p \Pi_i$. Since we are assuming continuous control, we have that $\bar{u}_i = u_i$.

With the setup described above, the authors in [10] show that the closed-loop system achieves output synchronization asymptotically.

Theorem 1 ([10, Theorem 5][‡])

If the graph \mathcal{G} is rooted and, for all $i \in \{1, \dots, N\}$, K_i and L_i are such that $A_i^p + B_i^p K_i$ and $A_i^p + L_i C_i^p$ are Hurwitz, respectively, then, for all $i \in \{1, \dots, N\}$ and all initial conditions $x_i^p(0) \in \mathbb{R}^{n_i^p}$, $x_i^c(0) \in \mathbb{R}^{n_i^p}$, and $\zeta_i(0) \in \mathbb{R}^m$, there exist $\kappa \geq 1$ and $\lambda > 0$ such that

$$\|z_i(t) - E_r e^{A_r t} (\beta^\top \otimes I_m) \zeta(0)\| \leq \kappa e^{-\lambda t} \|z_i(0) - E_r (\beta^\top \otimes I_m) \zeta(0)\| \quad (10)$$

for all $t \geq 0$, where $\zeta(0) = (\zeta_1(0), \dots, \zeta_N(0))$ and β is defined in Lemma 6 (Section A.1).

In the next section, we describe a control architecture that introduces event-triggered mechanisms in the communication links between agents and in the local output regulation controller, for which we prove boundedness of the tracking errors rather than asymptotic convergence to zero.

2.2. Proposed control architecture

Consider Figure 2 where the proposed control architecture for agent i is represented. It consists of a reference generator, an output regulation controller, and three event detectors. The setup is based on the one described in Section 2.1, except for the event detectors introduced and some additional state variables included in the reference generator. In what follows, we describe in detail the changes introduced.

The internal state of the output regulation controller denoted by x_i^c represents an estimate of the state of the plant x_i^p and of the exogenous disturbance w_i . The output regulation controller is a

[‡]Theorem 5 in [10] is actually more general since it proves asymptotic synchronization for time-varying graph topologies provided they are uniformly connected.

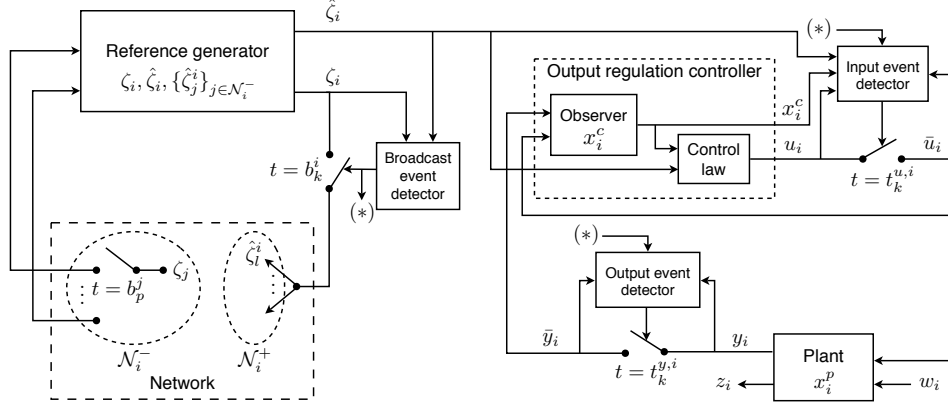


Figure 2. Proposed control architecture from the point of view of agent i . Note that this control system is distributed since all event detection blocks depend only on local signals available to agent i .

modified version of (8) and (9), where $x_i^c \in \mathbb{R}^{n_i^c}$ with $n_i^c = n_i^p + n_i^w$, satisfies, for all $t \geq 0$,

$$\dot{x}_i^c(t) = A_i^c x_i^c(t) + B_i^c \bar{u}_i(t) + L_i(C_i^c x_i^c(t) - \bar{y}_i(t)) \quad (11a)$$

$$u_i(t) = K_i^c x_i^c(t) + K_i^r \hat{\zeta}_i(t). \quad (11b)$$

The matrices involved in (11) are defined later in Section 3.2. The input and output event detectors operate independently of each other and continuously test their corresponding event triggering conditions. If the output event detector's triggering condition is violated, the signal \bar{y}_i is set to the current value of the output of plant y_i . Otherwise, \bar{y}_i remains constant. If the input event detector's triggering condition is violated, the signal \bar{u}_i is set to the current value of the output of the regulation controller u_i . Otherwise, \bar{u}_i remains constant. Thus, the signals \bar{y}_i and \bar{u}_i satisfy, for all $k \geq 0$,

$$\bar{y}_i(t) = y_i(t_k^{y,i}), \forall t \in [t_k^{y,i}, t_{k+1}^{y,i}) \quad (12a)$$

$$\bar{u}_i(t) = u_i(t_k^{u,i}), \forall t \in [t_k^{u,i}, t_{k+1}^{u,i}), \quad (12b)$$

where $\{t_k^{y,i}\}_{k \geq 0}$ and $\{t_k^{u,i}\}_{k \geq 0}$ are strictly increasing sequences that correspond to time instants when the output of the plant is sampled and to time instants when the control input is updated, respectively. Without loss of generality, we will assume henceforth that $t_0^{y,i} = t_0^{u,i} = 0$ for all $i \in \{1, \dots, N\}$. The sequences of sampling and update times are generated according to

$$t_{k+1}^{y,i} = \inf\{t > t_k^{y,i} : \mathbf{f}_i^y(y_i(t), \bar{y}_i(t), \bar{\tau}_i^y(t)) \text{ is true}\} \quad (13a)$$

$$t_{k+1}^{u,i} = \inf\{t > t_k^{u,i} : \mathbf{f}_i^u(\hat{\zeta}_i(t), x_i^c(t), u_i(t), \bar{u}_i(t), \bar{\tau}_i^u(t)) \text{ is true}\}, \quad (13b)$$

where \mathbf{f}_i^y and \mathbf{f}_i^u are functions that take values in the set $\{\text{true}, \text{false}\}$. The additional state variables $\bar{\tau}_i^y$ and $\bar{\tau}_i^u$ represent timers that are used to keep track of the time elapsed since the last event time. Their dynamics may be written in the form of an impulsive system[§] as

$$\begin{cases} \dot{\bar{\tau}}_i^y = 1, & t \in [t_k^{y,i}, t_{k+1}^{y,i}), \\ \bar{\tau}_i^y = 0, & t = t_k^{y,i}, \end{cases} \quad (14a)$$

$$\bar{\tau}_i^y = 0, \quad t = t_k^{y,i}, \quad (14b)$$

$$\begin{cases} \dot{\bar{\tau}}_i^u = 1, & t \in [t_k^{u,i}, t_{k+1}^{u,i}), \\ \bar{\tau}_i^u = 0, & t = t_k^{u,i}. \end{cases} \quad (15a)$$

$$\bar{\tau}_i^u = 0, \quad t = t_k^{u,i}. \quad (15b)$$

The output and input event detectors continuously evaluate \mathbf{f}_i^y and \mathbf{f}_i^u , respectively, until they become true meaning that a violation of the corresponding event condition has occurred and that a

[§]See Section A.2 for a definition of impulsive system and a list of references on the subject.

new sampling or update time must be triggered. Thus, for all $k \geq 0$, we have that

$$\begin{cases} \mathbf{f}_i^y(y_i(t_k^{y,i}), \bar{y}_i(t_k^{y,i}), \bar{\tau}_i^y(t_k^{y,i})) \text{ is false} \\ \mathbf{f}_i^u(\hat{\zeta}_i(t_k^{y,i}), x_i^c(t_k^{y,i}), u_i(t_k^{y,i}), \bar{u}_i(t_k^{y,i}), \bar{\tau}_i^u(t_k^{y,i})) \text{ is false.} \end{cases} \quad (16a)$$

$$\quad (16b)$$

If one can show that the sequences $\{t_k^{y,i}\}_{k \geq 0}$ and $\{t_k^{u,i}\}_{k \geq 0}$ do not have any accumulation points, then, for all $t \geq 0$, it will follow that

$$\begin{cases} \mathbf{f}_i^y(y_i(t), \bar{y}_i(t), \bar{\tau}_i^y(t)) \text{ is false} \\ \mathbf{f}_i^u(\hat{\zeta}_i(t), x_i^c(t), u_i(t), \bar{u}_i(t), \bar{\tau}_i^u(t)) \text{ is false.} \end{cases} \quad (17a)$$

$$\quad (17b)$$

This means that functions \mathbf{f}_i^y and \mathbf{f}_i^u are selected such that they are true for state configurations that are undesirable and that are avoided by triggering an event and executing the corresponding action (sampling the output or updating the control input). In Section 3, we address the single agent case to demonstrate how to select the controller matrices in (11) and the event functions \mathbf{f}_i^y and \mathbf{f}_i^u in (13), such that the tracking error $z_i - E_r \hat{\zeta}_i$ is bounded.

The other main component of the control architecture presented in Figure 2 is the reference generator, whose internal state is described by three elements: ζ_i , $\hat{\zeta}_i$, and $\hat{\zeta}_j^i$ with $j \in \mathcal{N}_i^-$.

The state ζ_i must evolve in such a way that its trajectory is (approximately) the same across all agents. The current value of ζ_i is broadcast to the out-neighbors of agent i whenever a given event-triggering condition (essentially a function of ζ_i and $\hat{\zeta}_i$) is violated. The sequence of time instants where this violation occurs is referred to as sequence of broadcast times of agent i and is denoted by $\{b_k^i\}_{k \geq 0}$ (where $b_0^i = 0$).

The state variable $\hat{\zeta}_i$ evolves according to the reference model between broadcast times of plant i and is reset to the current value of ζ_i when a broadcast occurs. The dynamics of $\hat{\zeta}_i$ may be written in the form of an impulsive system as

$$\begin{cases} \dot{\hat{\zeta}}_i = A_r \hat{\zeta}_i, & t \in [b_k^i, b_{k+1}^i), \\ \hat{\zeta}_i = \zeta_i^-, & t = b_k^i. \end{cases} \quad (18a)$$

$$\quad (18b)$$

The state $\hat{\zeta}_i$ is fed to the output regulation controller so that it can drive the regulated output of the plant z_i towards $E_r \hat{\zeta}_i$.

The additional states $\hat{\zeta}_j^i$ represent local replicas of the state ζ_j of agent i 's in-neighbors. The dynamics of $\hat{\zeta}_j^i$ are similar to those of $\hat{\zeta}_i$ except that when an in-neighbor of agent i , say $j \in \mathcal{N}_i^-$, broadcasts the current value of ζ_j , this value is used to reset the value of $\hat{\zeta}_j^i$, as modeled by the impulsive system

$$\begin{cases} \dot{\hat{\zeta}}_j^i = A_r \hat{\zeta}_j^i, & t \in [b_k^j, b_{k+1}^j), \\ \hat{\zeta}_j^i = \zeta_j^-, & t = b_k^j. \end{cases} \quad (19a)$$

$$\quad (19b)$$

The dynamics of ζ_i are as in (6) where, to avoid the need for continuous communication links among agents, instead of (7) v_i is defined as

$$v_i = \sum_{j=1}^N a_{ij} (\hat{\zeta}_j^i - \hat{\zeta}_i). \quad (20)$$

Without loss of generality, suppose that, for all $i, j \in \{1, \dots, N\}$, $\hat{\zeta}_j^i$ is initialized with the value $\zeta_j(0)$. Since $\hat{\zeta}_j$ and $\hat{\zeta}_j^i$ have the same dynamics (compare (18) with $i = j$ and (19)), we have that $\hat{\zeta}_j^i(t) = \hat{\zeta}_j(t)$ for all $t \geq 0$. Therefore, for analysis purposes, only the state variable $\hat{\zeta}_j$ is required and we may rewrite (20) as

$$v_i = \sum_{j=1}^N a_{ij} (\hat{\zeta}_j - \hat{\zeta}_i). \quad (21)$$

Note that if the broadcasted information were to arrive at each out-neighbor of agent i at different times due to, e.g., transmission delays, then the previous simplification would not be possible.

Finally, the sequence of broadcast times of agent i is generated according to

$$b_{k+1}^i = \inf\{t > b_k^i : |\hat{\zeta}_i(t) - \zeta_i(t)| \geq c(t)\}, \quad (22)$$

where $c(t)$ represents a non-negative time-varying threshold defined as $c(t) = c_0 + c_1 e^{-\alpha t}$, with $c_0, c_1, \alpha \geq 0$. The threshold starts at a value of $c_0 + c_1$ and then decreases monotonically, reaching c_0 asymptotically. Note that after a broadcast by agent i , we have that $|\hat{\zeta}_i(b_k^i) - \zeta_i(b_k^i)| = 0$. Assuming $\{b_k^i\}_{k \geq 0}$ does not have any accumulation points, the triggering condition in (22) ensures that $|\hat{\zeta}_i(t) - \zeta_i(t)| < c(t)$ for all $t \geq 0$. For reasons that will become clear in Section 4, after a broadcast is executed, a reset in the output and input event detectors of agent i has to be made.

Regarding the reference generator component, namely the subsystem formed by (6), (18), (19), and (21), the following is shown in [34].

Theorem 2 ([34, Theorem 3 and Lemma 3])

Let $\delta(t) = \zeta(t) - \mathbf{1}_N \otimes \zeta_0(t)$ for all $t \geq 0$ where $\zeta_0(0) = (\beta^\top \otimes I_m)\zeta(0)$. If \mathcal{G} is a rooted graph and

$$\Re\{\lambda + \mu\} < 0 \text{ for all } \lambda \in \sigma(A_r) \text{ and } \mu \in \sigma(\mathcal{L}) \setminus \{0\}, \quad (23)$$

then, for all initial conditions $\zeta(0) \in \mathbb{R}^{Nm}$, there exist $0 < \bar{\delta}_\infty \leq \bar{\delta}$ such that, for all $t \geq 0$,

$$\|\delta(t)\| \leq \bar{\delta} \text{ and } \lim_{t \rightarrow +\infty} \|\delta(t)\| \leq \bar{\delta}_\infty. \quad (24)$$

Moreover, if $c_0 > 0$, then there exists $\theta_{\min} > 0$ such that $b_{k+1}^i - b_k^i \geq \theta_{\min}$ for all $k \geq 0$ and all $i \in \{1, \dots, N\}$.

Theorem 2 shows that the internal state of the reference generator of all agents converges to a neighborhood of the solution of (3) with initial condition $\zeta_0(0) = (\beta^\top \otimes I_m)\zeta(0)$, where the radius of the neighborhood is bounded by $\bar{\delta}$ and asymptotically bounded by $\bar{\delta}_\infty$.

In the next section, we start by addressing the output regulation problem for a single agent and leave the problem of synchronizing multiple agents for Section 4.

3. EVENT-TRIGGERED OUTPUT REGULATION

As discussed in Section 2, one of the components required to achieve output synchronization is an event-triggered output regulation controller that can guarantee boundedness of the tracking error. In this section, we propose a solution inspired by the work reported in [35] developed originally for event-triggered stabilization of LTI plants.

3.1. Problem formulation

In Figure 3 we have isolated the components of the control architecture introduced in Figure 2 that are relevant to the output regulation problem.[¶] In this setup, the reference generator has been replaced by an exosystem with state $x_r \in \mathbb{R}^{n_r}$ and initial state $x_r(0)$ that satisfies, for all $t \geq 0$,

$$\dot{x}_r = A_r x_r \quad (25a)$$

$$z_r = E_r x_r, \quad (25b)$$

where $E_r \in \mathbb{R}^{n_z \times n_r}$. Thus, the tracking error is defined, for all $t \geq 0$, as

$$e_r(t) = z(t) - z_r(t). \quad (26)$$

[¶]In this section, since we are only addressing a single agent, to avoid unnecessary complexity we simplify the notation by dropping i as a subscript or superscript, depending on the situation, and moving the superscripts to subscripts when possible (for example, x_i^p , y_i , and $t_k^{y,i}$ become x_p , y , and t_k^y , respectively).

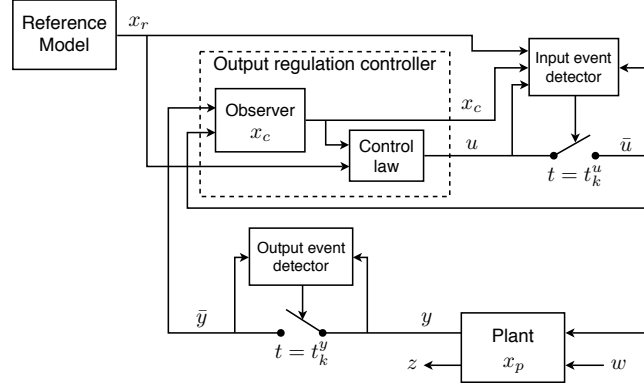


Figure 3. Control architecture for event-triggered output regulation.

For convenience, the disturbance model and reference model states are collected in $\psi = (w, x_r) \in \mathbb{R}^{n_\psi}$ whose dynamics are given by

$$\dot{\psi} = S\psi \quad (27)$$

where $S = \text{diag}(A_w, A_r)$. The hold behavior defined by (12) may be equivalently described by the impulsive systems

$$\begin{cases} \dot{\bar{y}} = 0, & t \in [t_k^y, t_{k+1}^y), \\ \bar{y} = y^-, & t = t_k^y, \end{cases} \quad (28a)$$

$$\bar{y} = y^-, \quad t = t_k^y, \quad (28b)$$

$$\begin{cases} \dot{\bar{u}} = 0, & t \in [t_k^u, t_{k+1}^u), \\ \bar{u} = u^-, & t = t_k^u, \end{cases} \quad (29a)$$

$$\bar{u} = u^-, \quad t = t_k^u, \quad (29b)$$

where $\bar{y}(0) = y(0)$ and $\bar{u}(0) = u(0)$. Errors induced by these hold devices are represented by $\tilde{y} = \bar{y} - y$ and $\tilde{u} = \bar{u} - u$. For a more compact notation, we introduce the variables $\mu = (y, u) \in \mathbb{R}^{n_\mu}$, $\bar{\mu} = (\bar{y}, \bar{u})$, and $\tilde{\mu} = \bar{\mu} - \mu$.

To solve the output regulation problem, we consider dynamic controllers of the form

$$\dot{x}_c = \bar{A}_c x_c + \bar{B}_c \mu + \bar{E}_c \tilde{\mu} \quad (30a)$$

$$u = \bar{C}_c x_c + \bar{D}_c x_r, \quad (30b)$$

where $x_c \in \mathbb{R}^{n_c}$ is the state of the controller (\bar{A}_c , \bar{B}_c , \bar{E}_c , \bar{C}_c , and \bar{D}_c are matrices of appropriate dimensions). In a continuous-time setup, we have $\tilde{\mu} = 0$ and, in this case, we may take $\bar{E}_c = 0$. The term \bar{D}_c may be non-zero in situations where the reference state is known, which is the case here.

With continuous feedback between plant and controller, under some reasonable assumptions, there exists a controller that achieves asymptotic output regulation, that is, such that

$$\lim_{t \rightarrow +\infty} \|e_r(t)\| = 0. \quad (31)$$

With the proposed event-triggered output regulation controller, instead of asymptotic output regulation, we will prove boundedness of the tracking error where the bound depends on the magnitude of the reference state and of the exogenous disturbance. Namely, that, for all initial conditions, the tracking error is bounded for all $t \geq 0$ and satisfies

$$\lim_{t \rightarrow +\infty} \|e_r(t)\| \leq \rho \|\psi\|_{\mathcal{L}_\infty} \quad (32)$$

for some constant $\rho > 0$. Also, since the sampling and update intervals are not constant over time, we have to guarantee that no Zeno solutions occur. For (32) to be well defined, the state variable ψ has to satisfy $\|\psi\|_{\mathcal{L}_\infty} < \infty$, which restricts the eigenvalue structure of the matrices A_w and A_r . They are only allowed to have eigenvalues in the imaginary axis and each eigenvalue must have algebraic multiplicity equal to its geometric multiplicity, which is equivalent to the following assumption.

Assumption 1. Matrices A_w and A_r are skew-symmetric.

3.2. Proposed event-triggered output regulation controller

To derive the proposed event-triggered output regulation controller, we require the following standard assumptions of the output regulation problem in continuous-time.

Assumption 2. The pair (A_p, B_p) is stabilizable.

Assumption 3. The pair (A_p, E_p) and (A_c, C_c) are detectable, where

$$A_c = \begin{bmatrix} A_p & B_w \\ 0 & A_w \end{bmatrix} \text{ and } C_c = [C_p \quad C_w]. \quad (33)$$

Assumptions 2 and 3 are necessary to guarantee the existence of a stabilizing feedback law and of an asymptotic observer in continuous-time.

Assumption 4 (Regulator equations). There exist matrices $\Pi \in \mathbb{R}^{n_p \times n_\psi}$ and $\Gamma \in \mathbb{R}^{n_y \times n_\psi}$ such that

$$\Pi S = A_p \Pi + B_p \Gamma + [B_w \quad 0] \quad (34a)$$

$$\begin{bmatrix} 0 & E_r \end{bmatrix} = E_p \Pi, \quad (34b)$$

or, equivalently, that

$$\Pi_w A_w = A_p \Pi_w + B_p \Gamma_w + B_w \quad (35a)$$

$$\Pi_r A_r = A_p \Pi_r + B_p \Gamma_r \quad (35b)$$

$$0 = E_p \Pi_w \quad (35c)$$

$$E_r = E_p \Pi_r, \quad (35d)$$

where $\Pi = [\Pi_w \quad \Pi_r]$ and $\Gamma = [\Gamma_w \quad \Gamma_r]$.

This assumption guarantees that tracking of the desired reference model is possible for the given plant. Further details on the regulator equations may be found in [13, Chapter 1] and [14, Chapter 2], including additional assumptions that guarantee that (34) has a unique solution pair (Π, Γ) .

To solve the output regulation problem, an observer based dynamic controller is proposed with internal state $x_c \in \mathbb{R}^{n_c}$, with $n_c = n_p + n_w$, and dynamics given by

$$\dot{x}_c = A_c x_c + B_c \bar{u} + L(C_c x_c - \bar{y}) \quad (36a)$$

$$u = K_c x_c + K_r x_r \quad (36b)$$

where

$$B_c = \begin{bmatrix} B_p \\ 0 \end{bmatrix} \text{ and } K_c = [K_p \quad K_w]. \quad (37)$$

The state x_c represents an estimate of both the state of the plant x_p and of the disturbance w . The gain matrices K_p and L are such that $A_p + B_p K_p$ and $A_c + L C_c$ are Hurwitz. The remaining gain matrices are defined as

$$K_w = \Gamma_w - K_p \Pi_w \quad (38)$$

$$K_r = \Gamma_r - K_p \Pi_r. \quad (39)$$

The controller in (36) may be written as in (30) where

$$\bar{A}_c = A_c + L C_c, \bar{B}_c = \bar{E}_c = \begin{bmatrix} -L C_c \\ B_c \end{bmatrix}, \bar{C}_c = K_c, \text{ and } \bar{D}_c = K_r. \quad (40)$$

3.3. Synchronous event detector

Instead of addressing directly the problem with asynchronous event mechanisms as in (13), we will first consider the synchronous case where the output of the plant and the control input are sampled and updated, respectively, at the same time instant. In this case, we have $t_k^y = t_k^u = t_k$ for all $k \geq 0$ and we refer to $\{t_k\}_{k \geq 0}$ as the sequence of sampling times, which are generated according to

$$t_{k+1} = \inf\{t > t_k : \mathbf{f}(y(t), \bar{y}(t), x_r(t), x^c(t), u(t), \bar{u}(t), \bar{\tau}(t)) \text{ is true}\} \quad (41)$$

where \mathbf{f} is a function to be defined and the timer variable $\bar{\tau}$ can be either $\bar{\tau}_y$ or $\bar{\tau}_y$, since they are identical in the synchronous case. The hold behavior defined by (12) is, in the synchronous case, described by the impulsive system

$$\begin{cases} \dot{\bar{\mu}} = 0, & t \in [t_k, t_{k+1}), \\ \bar{\mu} = \mu^-, & t = t_k, \end{cases} \quad (42a)$$

$$(42b)$$

where $\bar{\mu}(0) = \mu(0)$.

To determine the function \mathbf{f} in (41), we need to analyze the error dynamics associated with the closed-loop system. Consider a change of coordinates defined as

$$\tilde{x}_p = x_p - \Pi \begin{bmatrix} w \\ x_r \end{bmatrix}, \tilde{x}_c = x_c - \begin{bmatrix} x_p \\ w \end{bmatrix}, \quad (43)$$

and let $\tilde{x} = (\tilde{x}_p, \tilde{x}_c) \in \mathbb{R}^{n_{\tilde{x}}}$ denote the error state. Merging (1), (2), (25), (36), and (42), the closed-loop dynamics may be written in compact form as an impulsive system with state $\xi = (\tilde{x}, \psi, \bar{\mu})$ and initial state $\xi(0) = (\tilde{x}(0), \tilde{x}_c(0), 0)$, that satisfies, for all $t \geq 0$,

$$\begin{cases} \dot{\xi} = \bar{A}\xi, & t \in [t_k, t_{k+1}), \\ \xi = \text{diag}(I_{n_{\tilde{x}}+n_{\psi}}, 0_{n_{\mu}})\xi^-, & t = t_k, \end{cases} \quad (44a)$$

$$(44b)$$

where

$$\bar{A} = \begin{bmatrix} F & G \\ -HF & -HG \end{bmatrix}, F = \begin{bmatrix} A_0 & 0 \\ 0 & S \end{bmatrix}, A_0 = \begin{bmatrix} A_p + B_p K_p & BK_c \\ 0 & A_c + LC_c \end{bmatrix}, \quad (45a)$$

$$G = \begin{bmatrix} G_0 \\ 0 \end{bmatrix}, G_0 = \begin{bmatrix} 0 & B_p \\ -L & 0 \end{bmatrix}, H = \begin{bmatrix} C_p & 0 & C_p \Pi + [C_w & 0] \\ K_p & K_c & \Gamma \end{bmatrix}. \quad (45b)$$

In particular, we may extract from (44) the dynamics of \tilde{x} . For all $t \geq 0$, \tilde{x} satisfies

$$\begin{cases} \dot{\tilde{x}} = A_0 \tilde{x} + G_0 \bar{\mu}, & t \in [t_k, t_{k+1}), \\ \tilde{x} = \tilde{x}^-, & t = t_k. \end{cases} \quad (46a)$$

$$(46b)$$

Given $Q \succ 0$, since both $A_p + B_p K_p$ and $A_c + LC_c$ are Hurwitz, there exists $P \succ 0$ be such that

$$A_0^\top P + P A_0 + Q = 0. \quad (47)$$

Consider the function $V : \mathbb{R}^{n_{\tilde{x}}} \rightarrow \mathbb{R}_+$ defined as

$$V(\tilde{x}) = \tilde{x}^\top P \tilde{x}. \quad (48)$$

Using (46) and (47), the time derivative of V satisfies, for all $t \in [t_k, t_{k+1})$,

$$\dot{V} = 2\tilde{x}^\top P(A_0 \tilde{x} + G_0 \bar{\mu}) \quad (49)$$

$$= -\tilde{x}^\top Q \tilde{x} + 2\tilde{x}^\top P G_0 \bar{\mu} \quad (50)$$

$$= -(1 - \sigma)\tilde{x}^\top Q \tilde{x} + \gamma^2 \psi^\top \psi + \xi^\top M_0 \xi \quad (51)$$

where $\sigma \in (0, 1)$ and

$$M_0 = \begin{bmatrix} -\sigma Q & 0 & PG_0 \\ 0 & -\gamma^2 I_{n_\psi} & 0 \\ * & 0 & 0 \end{bmatrix}. \quad (52)$$

If the controller is able to guarantee that, for all $t \geq 0$,

$$\xi^\top M_0 \xi \leq 0, \quad (53)$$

then, for all $t \geq 0$,

$$\dot{V} \leq -(1 - \sigma) \tilde{x}^\top Q \tilde{x} + \gamma^2 \psi^\top \psi. \quad (54)$$

Inequality (54) is important since it can be used to establish some of the stability properties of the closed-loop system.

Lemma 1

Suppose (53) is satisfied for all $t \geq 0$ and that the closed-loop system does not exhibit Zeno solutions. Then, for all initial conditions $x_p(0) \in \mathbb{R}^{n_p}$, $x_c(0) \in \mathbb{R}^{n_c}$, and $\psi(0) \in \mathbb{R}^{n_\psi}$:

1. the error system (46) is ISS^{||} from input ψ to state \tilde{x} ;
2. the tracking error satisfies

$$\lim_{t \rightarrow +\infty} \|e_r(t)\| \leq \rho \|\psi\|_{\mathcal{L}_\infty} \quad (55)$$

where $\rho = \frac{\gamma}{\sqrt{\lambda}} \|\bar{E}P^{-1/2}\|$, with $\lambda = (1 - \sigma) \frac{\lambda_{\min}(Q)}{\lambda_{\max}(P)}$ and $\bar{E} = [E_p \ 0] \in \mathbb{R}^{n_z \times (n_p + n_c)}$.

Remark 1. Note that for the special case where $\psi \equiv 0$ ($\Leftrightarrow \psi(0) = 0$ and $S = 0$), the output regulation problem becomes a stabilization problem and Lemma 1 (namely, the ISS property) implies that the closed-loop system is asymptotically stable.

Remark 2. The definition of ρ in Lemma 1 shows that an arbitrarily small tracking error can be achieved by reducing γ (and therefore ρ) but, in general, this will lead to an increase in the average sampling rate.

At this point, to guarantee that (53) holds for all $t \geq 0$, one could envision a tentative triggering mechanism defined as

$$t_{k+1} = \inf\{t > t_k : \xi^\top M_0 \xi \geq 0\}. \quad (56)$$

In this case, we have the following lemma.

Lemma 2

If $\{t_k\}_{k \geq 0}$ is generated by (56), then (53) holds for all $t \geq 0$ and there exists $\tau_{\min} > 0$ such that the sampling intervals $\tau_k = t_{k+1} - t_k$ satisfy $\tau_k \geq \tau_{\min}$ for all $k \geq 0$. Moreover, the largest possible value for τ_{\min} is

$$\tau_{\min}^* = \inf\{s > 0 : h(s) = 0\} \quad (57)$$

where the function $h : \mathbb{R}_+ \rightarrow \mathbb{R}$ is defined as

$$h(s) = \lambda_{\max} \left\{ \begin{bmatrix} I \\ 0 \end{bmatrix}^\top e^{\bar{A}^\top s} M_0 e^{\bar{A} s} \begin{bmatrix} I \\ 0 \end{bmatrix} \right\}. \quad (58)$$

^{||} See Section A.3 for the definition of ISS.

The problem with the triggering mechanism in (56) is that x_p and w are not fully known (only partial observation is available through y) and therefore the triggering condition cannot be enforced by a controller that has only access to y , x_c , x_r , \tilde{y} , and \tilde{u} . Note that it can, nonetheless, be fulfilled by a periodic controller operating with a sampling period equal to τ_{\min} , that is, if $t_{k+1} = t_k + \tau_{\min}$, then (53) holds for all $t \geq 0$. To overcome the fact that x_p and w are not fully known, we follow the approach used in [35] that exploits the stability properties guaranteed by τ_{\min} with an event condition stricter than (53) but that depends only on signals available to the controller. The new event-triggering mechanism generates $\{t_k\}_{k \geq 0}$ according to

$$t_{k+1} = \min\{t \geq t_k : \bar{\tau}(t) \geq \tau_{\min} \wedge \phi^\top(t)M\phi(t) \geq 0\}, \quad (59)$$

where $\phi = (y, x_r, x_c, \tilde{\mu})$ represents all the variables that are available to the output regulation controller, τ_{\min} is selected such that $0 < \tau_{\min} \leq \tau_{\min}^*$, and M is a symmetric matrix to be defined. The first event condition in (59) guarantees that a minimum time interval of τ_{\min} has to elapse between consecutive sampling instants. In the second event condition of (59), the matrix M is chosen such that, for all $\xi \in \mathbb{R}^{n_\xi}$,

$$\xi^\top M_0 \xi \leq \phi^\top M \phi \quad (60)$$

(note that ϕ can be obtained from ξ , that is, $\phi = V\xi$ for some matrix V).

Lemma 3

If $\{t_k\}_{k \geq 0}$ is generated by (59), then (53) holds for all $t \geq 0$.

In what follows, we show how to find a symmetric matrix M such that (60) holds. To make explicit the dependance of $\xi^\top M_0 \xi$ on known and unknown state variables, we perform a coordinate change. Let $\eta = (x_p, w, x_r, x_c, \tilde{\mu})$. Note that $\xi = T\eta$ where the matrix T is defined as

$$T = \begin{bmatrix} [I_{n_p} & -\Pi_w] & -\Pi_r & 0 & 0 \\ & -I_{n_c} & 0 & I_{n_c} & 0 \\ [0 & I_{n_w}] & 0 & 0 & 0 \\ & 0 & I_{n_r} & 0 & 0 \\ & 0 & 0 & 0 & I_{n_\mu} \end{bmatrix}. \quad (61)$$

Furthermore, for C_c defined in (33), there exists $C_c^\perp \in \mathbb{R}^{(n_c - n_y) \times n_c}$ such that $C_c^\perp C_c^\top = 0$ and $C_c^\perp (C_c^\perp)^\top = I_{n_c - n_y}$. Let $x_u \in \mathbb{R}^{n_c - n_y}$ be such that

$$\begin{bmatrix} x_u \\ y \end{bmatrix} = \begin{bmatrix} C_c^\perp \\ C_c \end{bmatrix} \begin{bmatrix} x_p \\ w \end{bmatrix}. \quad (62)$$

The variable x_u belongs to the subspace of \mathbb{R}^{n_c} that cannot be directly measured. Let

$$\widehat{Z}_c = \text{diag}(Z_c, I_{n_r + n_c + n_\mu}) \quad (63)$$

where

$$Z_c = \begin{bmatrix} C_c^\perp \\ C_c \end{bmatrix}^{-1} \quad (64)$$

(the matrix Z_c exists because C_c is assumed full row-rank). Then, we have that $\xi = T\eta = T\widehat{Z}_c\hat{\eta}$ where $\hat{\eta} = (x_u, y, x_r, x_c, \tilde{\mu}) = (x_u, \phi)$. Using this coordinate change, we obtain that

$$\xi^\top M_0 \xi = \hat{\eta}^\top \widehat{M}_0 \hat{\eta} \quad (65)$$

where $\widehat{M}_0 = (T\widehat{Z}_c)^\top M_0 T\widehat{Z}_c$. Note that, apart from x_u , all other elements of $\hat{\eta}$ are available to the controller. To eliminate the dependance of $\hat{\eta}^\top \widehat{M}_0 \hat{\eta}$ on x_u we resort to the Schur complement

technique (described in Section A.4), which yields

$$\hat{\eta}^\top \widehat{M}_0 \hat{\eta} \leq \phi^\top M \phi, \quad (66)$$

where M is the Schur complement of the appropriate sub-matrix of \widehat{M}_0 .**

With all the elements of the proposed event-triggered output regulation controller well defined, we are now ready to characterize its stability properties.

Theorem 3

Suppose Assumptions 1-4 are satisfied and consider the closed-loop system formed by the plant (1), the disturbance model (2), the reference system (25), the hold device (42), the output regulation controller (36), and the event mechanism (59). Then, for all initial conditions $x_p(0) \in \mathbb{R}^{n_p}$, $x_c(0) \in \mathbb{R}^{n_c}$, and $\psi(0) \in \mathbb{R}^{n_\psi}$:

1. the closed-loop system does not exhibit Zeno solutions;
2. the error system (46) is ISS from input ψ to state \bar{x} ;
3. the tracking error satisfies

$$\lim_{t \rightarrow +\infty} \|e_r(t)\| \leq \rho \|\psi\|_{\mathcal{L}_\infty} \quad (67)$$

where ρ is defined in Lemma 1.

As mentioned previously, the triggering mechanism in (59) is inspired by the work reported in [35] for output-feedback stabilization of LTI systems. Here, we have extended the results in [35] to the output regulation case. Moreover, we use a less conservative technique to derive the stricter condition (namely the Schur complement technique), thereby deriving a triggering mechanism that yields larger average sampling intervals while guaranteeing the same stability conditions (as shown in Example 1 of Section 3.6).

3.4. Asynchronous event detectors

In this section, we introduce the asynchronous operation of the output and input event detectors, by replacing (42) and (41) with (12) and (13), respectively. Asynchronous event-triggered mechanisms have been considered in [19, 35, 37–39]. Here, we follow the approach outlined in [35, 38] to derive the event functions \mathbf{f}_y and \mathbf{f}_u of the asynchronous event-triggering mechanism in (13) from the event function \mathbf{f} obtained for the synchronous case.

First, we partition the matrices G and H in (45) as

$$G = \begin{bmatrix} G_y & G_u \\ 0 & 0 \end{bmatrix} \text{ and } H = \begin{bmatrix} H_y \\ H_u \end{bmatrix}, \quad (68)$$

where

$$G_y = \begin{bmatrix} 0 \\ -L \end{bmatrix}, G_u = \begin{bmatrix} B_p \\ 0 \end{bmatrix}, H_y = [C_p \quad 0 \quad C_p \Pi + [C_w \quad 0]], \text{ and } H_u = [K_p \quad K_c \quad \Gamma]. \quad (69)$$

As pointed out in [35], given $\theta_u, \theta_y \geq 0$ such that $\theta_u + \theta_y = 1$, (53) holds if

$$\xi_y^\top \begin{bmatrix} -\theta_y \sigma Q & 0 & P G_y \\ 0 & -\theta_y \gamma^2 I_{n_\psi} & 0 \\ * & 0 & 0 \end{bmatrix} \xi_y \leq 0 \wedge \xi_u^\top \begin{bmatrix} -\theta_u \sigma Q & 0 & P G_u \\ 0 & -\theta_u \gamma^2 I_{n_\psi} & 0 \\ * & 0 & 0 \end{bmatrix} \xi_u \leq 0, \quad (70)$$

where $\xi_y = (\tilde{x}, \psi, \tilde{y})$ and $\xi_u = (\tilde{x}, \psi, \tilde{u})$. Unlike the previous section where we used the Schur complement technique on inequalities of this kind to eliminate the dependence on unknown

** See Section B.4 for a proof that the Schur complement technique may be applied to the matrix \widehat{M}_0 .

variables, in the case of asynchronous event mechanisms, the method used for variable elimination is more conservative. Instead of the conditions in (70), we consider stricter conditions. Namely, we have that (70) holds if

$$- \|\hat{\xi}\| \left(\theta_y \min\{\sigma\lambda_{\min}(Q), \gamma^2\} \|\hat{\xi}\| - 2\|PG_y\| \|\tilde{y}\| \right) \leq 0 \quad (71)$$

$$\wedge - \|\hat{\xi}\| \left(\theta_u \min\{\sigma\lambda_{\min}(Q), \gamma^2\} \|\hat{\xi}\| - 2\|PG_u\| \|\tilde{u}\| \right) \leq 0 \quad (72)$$

where $\hat{\xi} = (\tilde{x}, \psi)$, which in turn is equivalent to

$$\|\tilde{y}\| - w_y \|\hat{\xi}\| \leq 0 \wedge \|\tilde{u}\| - w_u \|\hat{\xi}\| \leq 0 \quad (73)$$

where $w_y = \theta_y \min\{\sigma\lambda_{\min}(Q), \gamma^2\} / (2\|PG_y\|)$ and $w_u = \theta_u \min\{\sigma\lambda_{\min}(Q), \gamma^2\} / (2\|PG_u\|)$. Let the sampling and update intervals be defined, for all $k \geq 0$, as $\tau_k^y = t_{k+1}^y - t_k^y$ and $\tau_k^u = t_{k+1}^u - t_k^u$, respectively. Unlike Section 3.3 where the minimum sampling interval could be computed exactly, for the case of asynchronous event mechanisms, only lower bounds on the minimum sampling and update intervals possible under condition (73) are provided.

Lemma 4

For $w, a, b, c \in \mathbb{R}_+$, let $s_{\min}(w, a, b, c)$ denote the smallest time instant $s > 0$ such that $\nu(s) = w$ where $\nu(t)$ satisfies $\nu(0) = 0$ and, for all $t \geq 0$,

$$\dot{\nu} = (c + \nu)(a + b\nu). \quad (74)$$

Suppose the sequences $\{t_k^y\}_{k \geq 0}$ and $\{t_k^u\}_{k \geq 0}$ are such that (73) holds for all $t \geq 0$. Then, for all $k \geq 0$, $\tau_k^y \geq \tau_{\min}^y$ and $\tau_k^u \geq \tau_{\min}^u$ where

$$\tau_{\min}^y = s_{\min}(w_y, \|F\| + w_u \|G_u\|, \|G_y\|, \|H_y\|) \quad (75a)$$

$$\tau_{\min}^u = s_{\min}(w_u, \|F\| + w_y \|G_y\|, \|G_u\|, \|H_u\|). \quad (75b)$$

Remark 3. The reason we did not apply the Schur complement technique to the matrices in (70) is that we do not have at this time a result similar to Lemma 4 for computing minimum sampling and update intervals when two triggering conditions based on generic quadratic forms operate asynchronously.

Again, a tentative triggering mechanism would be

$$t_{k+1}^y = \min\{t \geq t_k^y : \|\tilde{y}(t)\| - w_y \|\hat{\xi}(t)\| \geq 0\} \quad (76a)$$

$$t_{k+1}^u = \min\{t \geq t_k^u : \|\tilde{u}(t)\| - w_u \|\hat{\xi}(t)\| \geq 0\}, \quad (76b)$$

but, as can be seen, the conditions in (76) cannot be readily implemented by the output and input event detectors since they depend on variables that are not available to either one. To eliminate this dependence, we proceed as follows. Let $\eta_y = (x_u, y, x_r, x_c)$ and $\eta_u = (x_p, w, x_r, x_c)$, which represent the variables made available to the output and input event detectors, respectively. We have that $\hat{\xi} = T_y \eta_y$ and $\hat{\xi} = T_u \eta_u$ where T_y and T_u are appropriate sub-matrices of $T\hat{Z}_c$ and T , respectively. Note that T_y and T_u are invertible and therefore $T_y^\top T_y$ and $T_u^\top T_u$ are positive definite. Since any principal sub-matrix of a positive definite matrix is positive definite, we may apply the Schur complement technique to the matrices $T_y^\top T_y$ and $T_u^\top T_u$ to obtain symmetric matrices \widehat{M}_y and \widehat{M}_u , respectively, such that, for all $\hat{\xi} \in \mathbb{R}^{n_p + n_c + n_\psi}$,

$$\hat{\xi}^\top \hat{\xi} \geq y^\top \widehat{M}_y y \quad (77a)$$

$$\hat{\xi}^\top \hat{\xi} \geq \begin{bmatrix} x_r \\ x_c \end{bmatrix}^\top \widehat{M}_u \begin{bmatrix} x_r \\ x_c \end{bmatrix}. \quad (77b)$$

We conclude that (73) holds if

$$\tilde{y}^\top \tilde{y} - w_y^2 \left(y^\top \widehat{M}_y y \right) \leq 0 \wedge \tilde{u}^\top \tilde{u} - w_u^2 \left(\begin{bmatrix} x_r \\ x_c \end{bmatrix}^\top \widehat{M}_u \begin{bmatrix} x_r \\ x_c \end{bmatrix} \right) \leq 0. \quad (78)$$

Let $\phi_y = (y, \tilde{y})$, $\phi_u = (x_r, x_c, \tilde{u})$, $M_y = \text{diag}(-w_y^2 \widehat{M}_y, I_{n_y})$, and $M_u = \text{diag}(-w_u^2 \widehat{M}_u, I_{n_u})$. Then, the sequence of sampling and update times are generated according to

$$t_{k+1}^y = \min\{t \geq t_k^y : \tau_y(t) \geq \tau_{\min}^y \wedge \phi_y^\top(t) M_y \phi_y(t) \geq 0\} \quad (79a)$$

$$t_{k+1}^u = \min\{t \geq t_k^u : \tau_u(t) \geq \tau_{\min}^u \wedge \phi_u^\top(t) M_u \phi_u(t) \geq 0\}, \quad (79b)$$

where τ_{\min}^y and τ_{\min}^u are defined in (75).

Lemma 5

If $\{t_k^y\}_{k \geq 0}$ and $\{t_k^u\}_{k \geq 0}$ are generated by (79), then (53) holds for all $t \geq 0$.

Next, we prove the analogous version of Theorem 3 for the setup with asynchronous event detectors.

Theorem 4

Suppose Assumptions 1-4 are satisfied and consider the closed-loop system formed by the plant (1), the disturbance model (2), the reference system (25), the hold devices (28) and (29), the output regulation controller (36), and the event mechanism (79). Then, for all initial conditions $x_p(0) \in \mathbb{R}^{n_p}$, $x_c(0) \in \mathbb{R}^{n_c}$, and $\psi(0) \in \mathbb{R}^{n_\psi}$:

1. the closed-loop system does not exhibit Zeno solutions;
2. the error system (46) is ISS from input ψ to state \tilde{x} ;
3. the tracking error satisfies

$$\lim_{t \rightarrow +\infty} \|e_r(t)\| \leq \rho \|\psi\|_{\mathcal{L}_\infty} \quad (80)$$

where ρ is defined in Lemma 1.

3.5. A connection with threshold triggering

Consider again the synchronous triggering mechanism in (59) analyzed in Section 3.3. If instead of (53) the controller is able to guarantee that, for all $t \in [t_k, t_{k+1})$,

$$\xi^\top M_0 \xi \leq \varepsilon^2, \quad (81)$$

where ε is a positive constant, then, instead of (54), we have that, for all $t \geq 0$,

$$\dot{V} \leq -(1 - \sigma) \tilde{x}^\top Q \tilde{x} + \gamma^2 \psi^\top \psi + \varepsilon^2. \quad (82)$$

The constant ε is a design parameter that can be used to potentially reduce the average sampling rate observed by allowing a small violation of the original triggering condition. If the sampling times are generated by

$$t_{k+1} = \min\{t \geq t_k : \bar{\tau}(t) \geq \tau_{\min} \wedge \xi^\top M_0 \xi \geq \varepsilon^2\}, \quad (83)$$

it can be shown that, for all $t \geq 0$,

$$\|\tilde{x}(t)\| \leq e^{-\frac{1}{2}\lambda t} \sqrt{\frac{\lambda_{\max}(P)}{\lambda_{\min}(P)}} \|\tilde{x}(0)\| + \frac{\gamma}{\sqrt{\lambda_{\min}(P)\lambda}} \|\psi\|_{\mathcal{L}_\infty} + \frac{\varepsilon}{\sqrt{\lambda_{\min}(P)\lambda}} \quad (84)$$

$$= \beta(t, \|\tilde{x}(0)\|) + \rho_0 (\|\psi\|_{\mathcal{L}_\infty}) + \rho_1(\varepsilon). \quad (85)$$

This shows that (46) is input-to-state practically stable (ISpS)^{††} from ψ to \tilde{x} . The bound on the tracking error then becomes

$$\lim_{t \rightarrow +\infty} \|e_r(t)\| \leq \rho \|\psi\|_{\mathcal{L}_\infty} + \frac{\varepsilon}{\sqrt{\lambda}} \left\| \bar{E}P^{-1/2} \right\|, \quad (86)$$

where ρ is defined in Theorem 3. One could derive an expression similar to (57) to compute the minimum sampling interval for a given $\varepsilon > 0$ but it would require a bound on $\|\psi(t)\|$. It is simpler to use $\tau_{\min} = \tau_{\min}^*$ as defined in (57), instead of computing the actual minimum sampling interval for $\varepsilon > 0$, since τ_{\min}^* is already a lower bound on the minimum sampling interval achievable with $\varepsilon > 0$.

The inclusion of ε allows us to illustrate a relationship between threshold triggering and the triggering conditions obtained by applying the procedure used in Section 3.3 to eliminate variables from the triggering condition in (56). We define threshold triggering as enforcing, for all $t \in [t_k, t_{k+1})$, the condition

$$\|\tilde{\mu}\| \leq \hat{\varepsilon} \quad (87)$$

for some constant $\hat{\varepsilon} > 0$. This is a typical event-triggering condition designed to keep the error induced by sampling bounded. See [18, 40, 41] for some examples of this sort of triggering mechanism. If we eliminate \tilde{x} , w , x_r , and x_c from the triggering condition in (81) using the Schur complement technique, we are left with a condition on the error $\tilde{\mu}$ of the form

$$\tilde{\mu}^\top \tilde{M} \tilde{\mu} \leq \varepsilon^2. \quad (88)$$

Using the fact that $\tilde{\mu}^\top \tilde{M} \tilde{\mu} \leq \lambda_{\max}(\tilde{M}) \|\tilde{\mu}\|^2$, we conclude that (87) with

$$\hat{\varepsilon} = \frac{\varepsilon}{\sqrt{\lambda_{\max}(\tilde{M})}} \quad (89)$$

implies (88), which in turn implies (81). This shows that if the sampling times are generated by

$$t_{k+1} = \min\{t \geq t_k : \bar{\tau}(t) \geq \tau_{\min} \wedge \|\tilde{\mu}(t)\| \geq \hat{\varepsilon}\}, \quad (90)$$

then (81) will hold for all $t \geq 0$. However, given that the same stability properties are guaranteed, the sampling rate with (90) will be higher than necessary since (87) is stricter than (81).

3.6. Examples

In this section, we present three examples that illustrate the implementation of the proposed event-triggered output regulation controller and support the claims made in the previous sections.

Example 1 In this example, we consider a stabilization problem where the goal is to drive the state of the plant to the origin. The reference trajectory is thus identically zero and there are no disturbances present. In this case, the error state becomes simply $\tilde{x} = (x_p, x_c - x_p)$ since the observer only has to estimate x_p . We compare the triggering methods presented in [35] with synchronous and asynchronous event detectors (referred to in [35] as Architecture II and Architecture III, respectively), with the triggering methods proposed in the Section 3.3 and Section 3.4.

In the case of stabilization, the asynchronous triggering method presented in (79) is essentially the same as [35, Arch. III]. One difference is that, to derive the triggering conditions, instead of using the inequalities in (77), in [35] the authors use

$$\tilde{x}^\top \tilde{x} \geq \frac{1}{\|C_p\|} y^\top y \text{ and } \tilde{x}^\top \tilde{x} \geq \frac{1}{2} x_c^\top x_c \quad (91)$$

^{††}See Section A.3 for the definition of ISpS.

Table I. Statistics regarding the sequences of event times in Example 1.

Triggering method	Sampled variable	Computed minimum (ms)	Observed minimum (ms)	Observed average (ms)	Observed maximum (ms)
[35, Arch. II] $\theta_1 = 1, \theta_2 = 0$	(x_c, y)	0.576	0.576	3.98	11.6
(59)	(x_c, y)	3.74	6.24	28.6	221
[35, Arch. III] $\theta_1 = 0.5, \theta_2 = 0.5$	x_c	1.02	1.02	4.07	20.5
	y	0.477	0.477	1.55	8.85
(79)	u	1.02	1.02	10.9	147
$\theta_y = 0.5, \theta_u = 0.5$	y	0.477	0.477	1.54	73.4

(note that $\hat{\xi} = \tilde{x}$). However, this is irrelevant for this example since $\widehat{M}_u = \frac{1}{2}I_2$ and $\widehat{M}_y = (C_p C_p^\top)^{-1} = 1$, and therefore (77) reduces to (91). A second difference is that in [35, Arch. III] the input event detector holds the value of x_c instead of the value of u .

As in [35], the plant and controller gain matrices are

$$A_p = \begin{bmatrix} 2 & 3 \\ 1 & 3 \end{bmatrix}, B_p = \begin{bmatrix} 0 \\ 1 \end{bmatrix}, C_p = [1 \quad 0], K_p = [-15 \quad -10], L = \begin{bmatrix} -10 \\ -14 \end{bmatrix}, Q = I_4. \quad (92)$$

We set $\gamma = 0$ and select $\sigma = 0.95$, which yields a desired rate of decay of $\lambda = 4.26 \times 10^{-3}$. The initial conditions are $x_p(0) = [2 \quad 3]^\top$ and $x_c(0) = [0 \quad 0]^\top$. Regarding triggering parameters, Arch. II and Arch. III in [35] require two positive scalar parameters θ_1 and θ_2 that satisfy $\theta_1 + \theta_2 = 1$. The values selected in this example are $(\theta_1, \theta_2) = (1, 0)$ for Arch. II and $(\theta_1, \theta_2) = (0.5, 0.5)$ for Arch. III. For our asynchronous triggering method, we select $(\theta_u, \theta_y) = (0.5, 0.5)$ to match the choice made for the Arch. III method.

Simulation results are presented in Figure 4. Figure 4a shows the evolution of the Lyapunov function $V(t)$, which tends to zero in all cases as expected. The sequences of sampling intervals obtained for the synchronous cases are plotted in Figure 4b, while the sequences of sampling and update intervals obtained for the asynchronous cases are plotted in Figure 4c and Figure 4d. Statistics regarding the sequences of event times are given in Table I.

In the synchronous case, note that the minimum sampling interval given by (57) is $\tau_{\min}^* = 3.74$ ms, which is already very close to the observed average sampling interval of 3.98 ms obtained using [35, Arch. II]. The observed average sampling interval with (59) is 28.57 ms that is more than seven times greater than the one obtained with [35, Arch. II], while guaranteeing the same rate of decay. We can see in Figure 4a that, while the event-triggered controller is designed to enforce a rate of decay of λ , the actual rate of decay is higher.

In the asynchronous case, [35, Arch. III] and (79) produce similar results in the evolution of $V(t)$ and in the statistics of the sampling and update sequences, although the input event detector of (79) operating on u achieves a larger average update interval than the event detector of [35, Arch. III] operating on x_c .

Example 2 Consider the same plant of Example 1 and suppose the regulated output is equal to the measured output, that is, $E_p = C_p$. Also, an exogenous disturbance is included whose model is described by

$$A_w = \begin{bmatrix} 0 & -1 & 0 \\ 1 & 0 & 0 \\ 0 & 0 & 0 \end{bmatrix}, B_w = B_p [1 \quad 0 \quad 2], C_w = [0 \quad 1 \quad -1], \quad (93)$$

with initial condition $w(0) = [0.1 \quad 0 \quad 1]^\top$. This generates an input disturbance of the form $0.1 \cos(t) + 2$ and an output disturbance of the form $0.1 \sin(t) - 1$. The reference system is

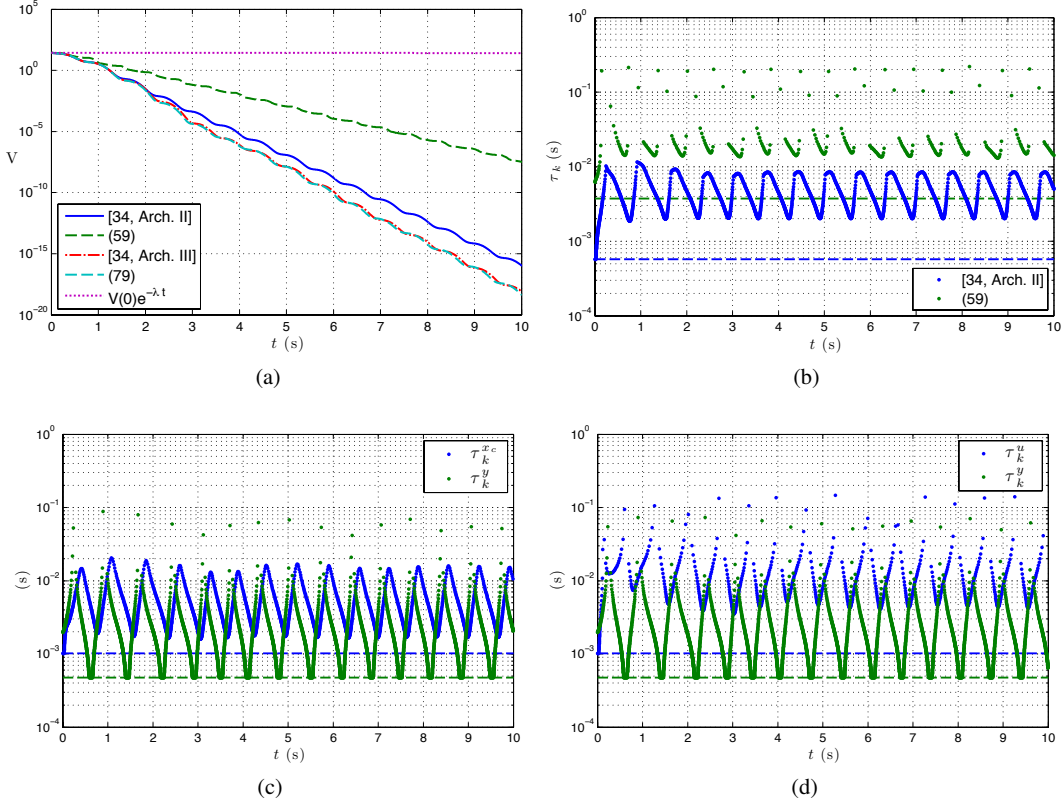


Figure 4. Simulation results for Example 1. (a) Evolution of the Lyapunov function V . (b) Sequences of sampling intervals $\{\tau_k\}_{k \geq 0}$ generated by [35, Arch. II] and (59) (the dashed lines represent the minimum sampling intervals defined in [35, Theorem 1] and (57)). (c) Sequences of sampling and update intervals $\{\tau_k^y\}_{k \geq 0}$ and $\{\tau_k^{x_c}\}_{k \geq 0}$ generated by [35, Arch. III] (the dashed lines represent the minimum sampling and update intervals defined in [35, Theorem 3]). (d) Sequences of sampling and update intervals $\{\tau_k^y\}_{k \geq 0}$ and $\{\tau_k^u\}_{k \geq 0}$ generated by (79) (the dashed lines represent the minimum sampling and update intervals defined in (75)).

described by

$$A_r = \begin{bmatrix} 0 & -1 & 1 & 0 \\ 1 & 0 & 0 & 1 \\ 0 & 0 & 0 & -\frac{1}{3} \\ 0 & 0 & \frac{1}{3} & 0 \end{bmatrix}, E_r = [1 \quad 0 \quad 1 \quad 0], \quad (94)$$

with initial condition $x_r(0) = [0 \quad 0 \quad 0 \quad 1]^\top$. This generates a periodic signal with two harmonic components, namely $z_r(t) = \frac{3}{2}(\cos(t) - \cos(\frac{t}{3})) - \sin(\frac{t}{3})$.

The controller gain K_p is obtained by solving an LQR control problem with weight matrices $Q_p = I_2$ and $R_p = 1$, that is, $K_p = -R_p^{-1}B_p^\top P_p$ where P_p is the positive definite solution of the algebraic Riccati equation

$$A_p^\top P_p + P_p A_p - P_p B_p R_p^{-1} B_p^\top P_p + Q_p = 0. \quad (95)$$

The observer gain L is computed in a similar manner and corresponds to the gain of a steady-state Kalman filter, that is, $L = -P_c C_c^\top R_c^{-1}$ where P_c is the positive definite solution of the algebraic Riccati equation

$$A_c P_c + P_c A_c^\top - P_c C_c^\top R_c^{-1} C_c P_c + Q_c = 0, \quad (96)$$

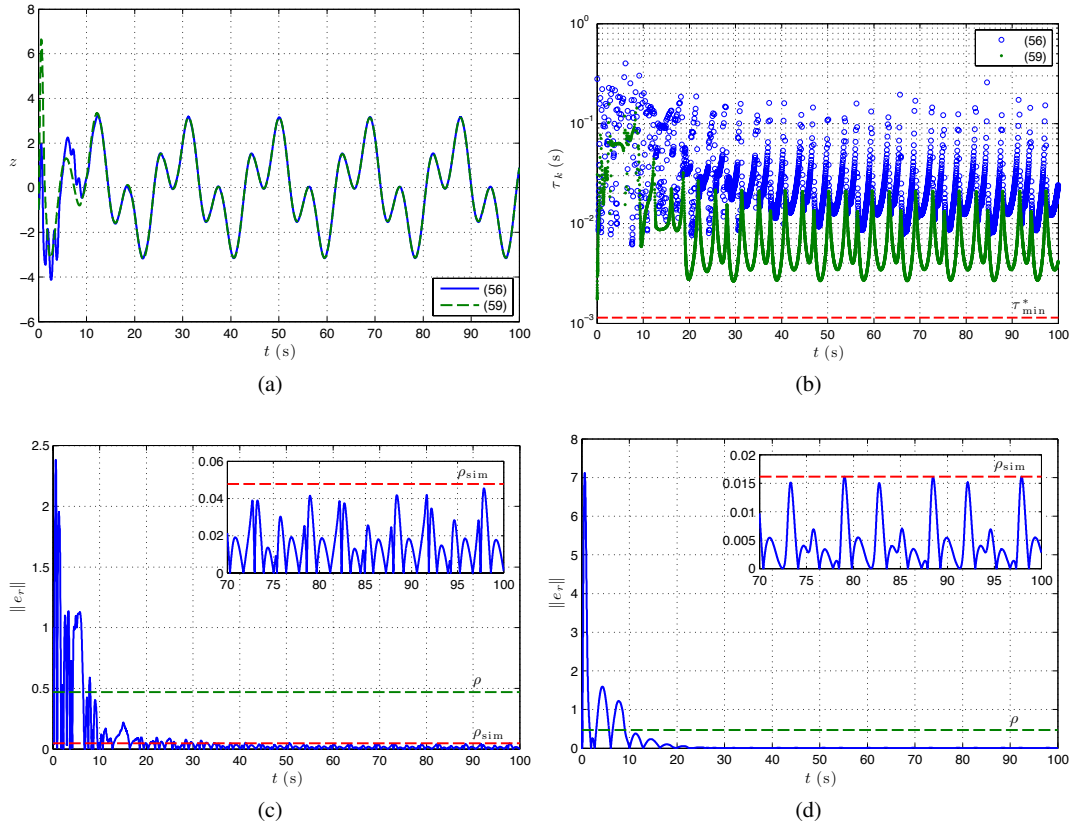


Figure 5. Simulation results for Example 2. (a) Trajectory of the regulated output of the plant z . (b) Sequence of sampling intervals $\{\tau_k\}_{k>0}$ and theoretical minimum sampling interval τ_{\min}^* . (c)-(d) Evolution of the norm of the tracking error e_r (with a zoom-in on the last 30 seconds of simulation), theoretical bound ρ , and estimated bound ρ_{sim} : (c) triggering method (56); (d) triggering method (59).

with $Q_c = 100I_5$ and $R_c = 1$. The remaining controller gains K_w and K_r are obtained from (38).

The initial conditions are $x_p(0) = [-1 \ 1]^T$ and $x_c(0) = 0$. The triggering parameters are $\sigma = 0.95$ and $\gamma = 0.025$, yielding a minimum sampling interval of $\tau_{\min}^* = 1.136$ ms computed from (57) and a bound on the tracking error of $\rho = 4.699 \times 10^{-1}$ computed from Theorem 3. The simulation results obtained for this example are presented in Figure 5. In Figure 5a, we have plotted the regulated output of the plant for each triggering method, which in both cases clearly converges to a neighborhood of the desired reference signal. The sequences of sampling intervals generated are shown in Figure 5b. As expected, the triggering method in (59) generates overall lower values for the sampling intervals when compared with (56), given that it is based on stricter but implementable triggering conditions. This fact is corroborated by the statistics given in Table II, where we have collected the minimum, maximum, and average sampling intervals observed in simulation, along with the computed minimum interval. In Figure 5d, we have plotted the trajectory of the tracking error and have included its theoretical bound ρ . For both triggering methods, the norm of the tracking error is well below the theoretical bound. We also include in Table II an estimate of the bound ρ based on the simulated data that we defined as

$$\rho_{\text{sim}} = \max_{50 \leq t \leq 100} \|e_r(t)\|, \quad (97)$$

where we try to remove the effect of transients due to initial conditions by ignoring the first 50 seconds of simulation data. We see that ρ_{sim} is one order of magnitude smaller than ρ , which seems to indicate that the expression derived for the latter may be conservative.

Table II. Statistics on the sequence of sampling intervals $\{\tau_k\}_{k \geq 0}$, computed over the whole simulation interval ($t \in [0, 100]$) and after transients ($t \in [50, 100]$), and estimated bound ρ_{sim} on the norm of the tracking error (Example 2).

Triggering method	Computed minimum (ms)	Observed						ρ_{sim}
		minimum (ms)		average (ms)		maximum (ms)		
		[0, 100]	[50, 100]	[0, 100]	[50, 100]	[0, 100]	[50, 100]	
(56)	1.136	6.159	7.770	18.30	22.56	258.7	401.0	4.78×10^{-2}
(59)	1.136	1.753	2.679	5.582	4.866	156.7	21.26	1.61×10^{-2}

Example 3 To illustrate the event-triggered output regulation controller with asynchronous event detectors, we consider a different plant but with the same reference and disturbance models of Example 2. The plant matrices are

$$A_p = \begin{bmatrix} 0.5 & -0.4 \\ 0.3 & -0.7 \end{bmatrix}, B_p = \begin{bmatrix} 0 \\ 1 \end{bmatrix}, C_p = E_p = \begin{bmatrix} 1 & 0 \end{bmatrix}. \quad (98)$$

The controller gains are selected as described in Example 2 by taking $Q_p = I_2$, $R_p = 1$, $Q_c = I_5$, and $R_c = 1$. The triggering parameters are $Q = I_4$, $\sigma = 0.95$, $\gamma = 1$, $\theta_y = 0.75$, and $\theta_u = 0.25$, yielding $\tau_{\min}^y = 0.965$ ms and $\tau_{\min}^u = 0.8389$ ms computed from (75) and a bound on the tracking error of $\rho = 5.558$.

The simulation results obtained are presented in Figure 6. Shown in Figures 6a and 6b are the trajectories of the regulated output and of the tracking error, respectively. It is clear that the controller with sampling and update times generated by (79) is able to follow the desired reference signal with a tracking error overall smaller than the one obtained when sampling and update times are generated according to (76). Consider in the particular the sequence of sampling intervals $\{\tau_k^y\}_{k \geq 0}$ generated by (79a) and represented in Figure 6c. Note that the sampling intervals repeatedly approach and equal the minimum sampling interval τ_{\min}^y . This occurs whenever the output of the plant y approaches zero (making the term $y^\top y$ in (79a) close to zero), generating a sequence of ever decreasing sampling intervals that are eventually equal to τ_{\min}^y before increasing again. The output event detector thus enters consistently a very conservative sampling regime that, although only lasts a small period of time, is enough to represent a substantial decrease in the average sampling interval when compared to the intervals generated by (76a). This decrease in the average sampling interval is clearly illustrated in Table III. Note that the above phenomena does not seem to occur for the sequence of update intervals $\{\tau_k^u\}_{k \geq 0}$ represented in Figure 6d, possibly due to the fact that more information is available to the input event detector, namely the reference state x_r and the controller state x_c . The sequence $\{t_k^u\}_{k \geq 0}$ generated by (79b) thus retains approximately the same characteristics of the sequence generated by (76b).

One possible way of minimizing the decrease in the average sampling interval is to improve the bound τ_{\min}^y . Comparing the values of $\{\tau_k^y\}_{k \geq 0}$ generated by (76a) with τ_{\min}^y , we see that there appears to be some room for improvement. Another possibility, would be to try to adjust τ_{\min}^y by modifying the controller gains or the event parameters, but this would lead us to a trial-and-error approach for which it is hard to predict the outcome. Finally, another option already alluded to in Section 3.5, is to include an ϵ term in the event conditions. This strategy was used in [19] when addressing event-triggered stabilization of LTI plants, to circumvent a similar problem. To illustrate how the inclusion of ϵ modifies the closed-loop behavior, we present simulation results for the case where the sampling and update times are generated according to

$$t_{k+1}^y = \min\{t \geq t_k^y : \phi_y^\top(t) M_y \phi_y(t) \geq \epsilon^2\} \quad (99a)$$

$$t_{k+1}^u = \min\{t \geq t_k^u : \phi_u^\top(t) M_u \phi_u(t) \geq 0\}, \quad (99b)$$

where $\epsilon = 0.01$. Note that, in this case, the stability guarantees are different and the existence of a minimum sampling interval is not guaranteed (τ_{\min}^y and τ_{\min}^u are not valid any longer), although

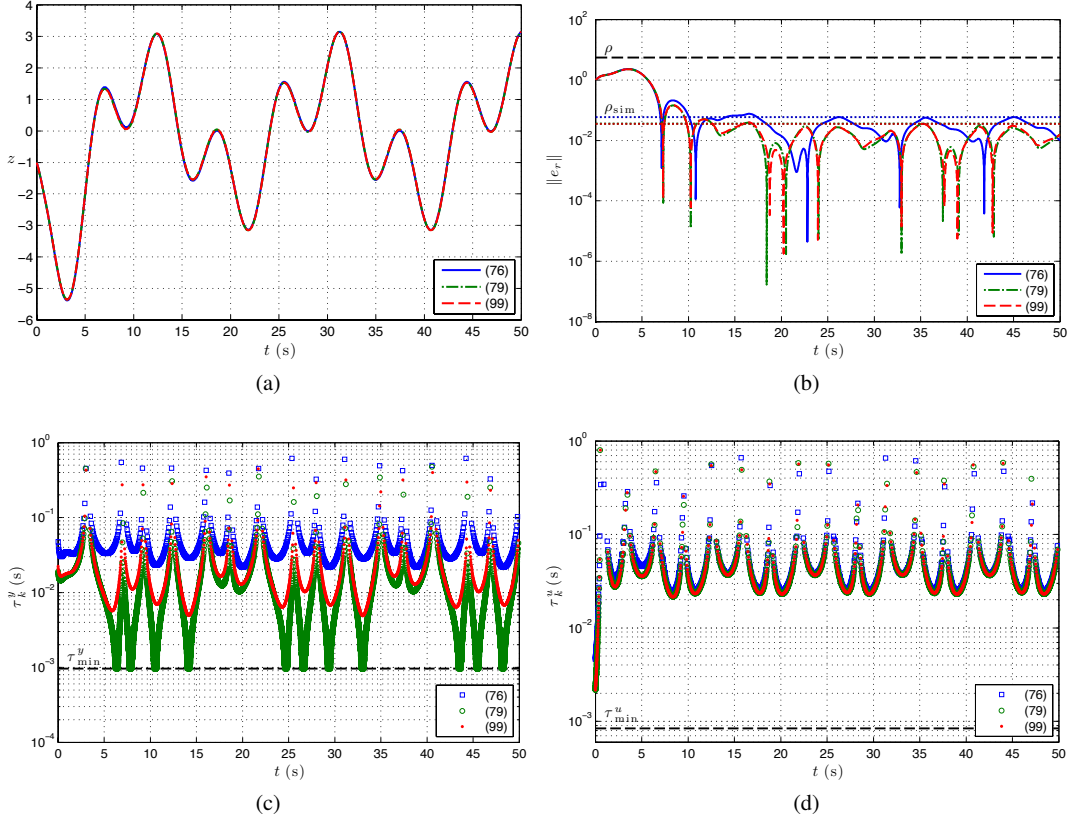


Figure 6. Simulation results for Example 3. (a) Trajectory of the regulated output of the plant z . (b) Evolution of the norm of the tracking error $e_r(t)$, theoretical bound ρ , and estimated bound ρ_{sim} . (c) Sequence of sampling intervals $\{\tau_k^y\}_{k \geq 0}$ and theoretical bound on the minimum sampling interval τ_{min}^y . (d) Sequence of update intervals $\{\tau_k^u\}_{k \geq 0}$ and theoretical bound on the minimum update interval τ_{min}^u .

Table III. Statistics on the sequences of sampling and update intervals ($\{\tau_k^y\}_{k \geq 0}$ and $\{\tau_k^u\}_{k \geq 0}$, respectively) and estimated bound on the norm of the tracking error ρ_{sim} (Example 3).

Triggering method	Event detector	Computed minimum (ms)	Observed			ρ_{sim}
			minimum (ms)	average (ms)	maximum (ms)	
(76)	output	0.965	21.87	43.18	617.8	5.95×10^{-2}
	input	0.839	4.589	44.71	659.8	
(79)	output	0.965	0.965	5.243	477.5	3.64×10^{-2}
	input	0.839	2.164	40.01	798.7	
(99)	output	—	4.922	14.57	448.5	3.57×10^{-2}
	input	—	2.164	39.95	797.3	

one can envision a modification of the results in [19] to prove this fact. The simulation results are presented in Figure 6. We see that the tracking error is essentially the same as the one obtained with (79) but $\{\tau_k^y\}_{k \geq 0}$ avoids the periods of small sampling intervals, which leads to a larger average sampling interval, as made clear in Table III.

This example shows that in spite of the theoretical results guaranteeing certain stability properties, from an implementation perspective, there are some issues that deserve further attention. A possible avenue of research is to consider an hybrid triggering mechanism that combines the lower bounds on the minimum intervals used in (79) with the ϵ -technique employed in (99) and discussed in Section 3.5.

4. EVENT-TRIGGERED OUTPUT SYNCHRONIZATION

In this section, we combine the results of Section 3 with Theorem 2 to demonstrate that the proposed control architecture, described in Section 2.2 and depicted in Figure 2, solves the problem of event-triggered output synchronization of agents with heterogeneous LTI dynamics.

We assume that each agent satisfies Assumptions 1-4 of Section 3, so that the local output regulation controller and corresponding event detectors may operate as described in that same section. Keep in mind that the reference state x_r is replaced by $\hat{\zeta}_i$ provided by the reference generator. As for the reference generators, they operate as described in Section 2.2 where the communication graph \mathcal{G} is assumed to be rooted. The requirement that the unstable dynamics of A_r have to be dominated (that is, (23) must hold), is automatically satisfied since, by Assumption 1, the eigenvalues of A_r are all imaginary.

The only aspect of the proposed control architecture that has to be discussed at this point, is the need to reset the output and input event detectors after a broadcast of agent i has occurred. Formally, this means that extra reset conditions are added to the corresponding event detectors (namely in (14)-(15) and (28)-(29)) such that when $t = b_k^i$, we set $\bar{y}_i = y_i$, $\bar{\tau}_i^y = 0$, $\bar{u}_i = u_i$, and $\bar{\tau}_i^u = 0$. Sampling and updates times are still generated by (79), keeping in mind that $t_k^{y,i}$ and $t_k^{u,i}$ represent time instants where \mathbf{f}_i^y or \mathbf{f}_i^u are true, and do not include sampling or update times made due to a broadcast triggered by the reference generator (in other words, originated by the extra reset conditions introduced).

The reason for these extra reset conditions is related with the computation of the minimum sampling and update intervals of the output and input event detectors. There were two possibilities for the reference state provided by the reference generator to the output regulation controller: ζ_i or $\hat{\zeta}_i$. The state ζ_i is continuous for all $t \geq 0$ but predicting its evolution is difficult since its dynamics depend on state variables that change whenever new information arrives from neighboring agents (cf. (6) and (21)). On the other hand, $\hat{\zeta}_i$ follows the reference model dynamics between broadcast times of agent i but exhibits discontinuities at the broadcast times (cf. (18)). We decided to use $\hat{\zeta}_i$ as the reference state because of its simpler dynamics, and to avoid the discontinuity issue, we introduced the above mentioned extra reset conditions (otherwise, we would not have a guarantee that the minimum sampling and update intervals even existed). Had we used ζ_i as the reference state, deriving expressions for the minimum intervals could still be possible although they would be more involved and probably more conservative.

With all the elements of the proposed control architecture well defined, we are now ready to state our main result.

Theorem 5

If each agent satisfies Assumptions 1-4 and the communication graph \mathcal{G} is rooted, then there exist $d > 0$ such that

$$\|z_i(t) - E_r e^{A_r t} (\beta^\top \otimes I_m) \zeta(0)\| \leq d \quad (100)$$

for all $t \geq 0$ and all $i \in \{1, \dots, N\}$. Moreover, the closed-loop system does not exhibit Zeno solutions.

Note that Theorem 5 also holds if the event detectors operate synchronously as described in Section 3.3.

4.1. Multi-agent example

In this section, we illustrate the proposed event-triggered output synchronization controller on a group of $N = 6$ agents. The matrices associated with the dynamics of each agent are given in

Table IV. Parameters associated with the dynamics and the disturbances of each agent.

i	Σ_i	$x_i^p(0)$	A_i^w	w_0^i
1	$\begin{bmatrix} 0 & 1 & 0 & 0 & 0 \\ 0 & 0 & 1 & 0 & 0 \\ 2 & -4 & 2 & 1 & 1 \\ 1 & 0 & 0 & 0 & 0 \\ 1 & 0 & 0 & 0 & 0 \end{bmatrix}$	$\begin{bmatrix} 0.1000 \\ 0.0905 \\ 0.0810 \end{bmatrix}$	0	1
2	$\begin{bmatrix} 0 & 1 & 0 & 0 & 0 & 0 & 0 \\ 0 & 0 & 1 & 0 & 0 & 0 & 0 \\ 3 & -2 & 1 & 1 & 1 & 0 & 0 \\ 1 & 0 & 0 & 0 & 1 & -1 & 0 \\ 1 & 0 & 0 & 0 & 0 & 0 & 0 \end{bmatrix}$	$\begin{bmatrix} 0.0714 \\ 0.0619 \\ 0.0524 \end{bmatrix}$	$\begin{bmatrix} 0 & -1 & 0 \\ 1 & 0 & 0 \\ 0 & 0 & 0 \end{bmatrix}$	$\begin{bmatrix} 1 \\ 0 \\ 1 \end{bmatrix}$
3	$\begin{bmatrix} 0 & 1 & 0 & 0 & 0 & 0 & 0 \\ 0 & 0 & 1 & 0 & 0 & 0 & 0 \\ -1 & 2 & -3 & 1 & 1 & 0 & 0 \\ 0 & 1 & 0 & 0 & 1 & -1 & 0 \\ 1 & 0 & 0 & 0 & 0 & 0 & 0 \end{bmatrix}$	$\begin{bmatrix} 0.0429 \\ 0.0333 \\ 0.0238 \end{bmatrix}$	$\begin{bmatrix} 0 & -1 & 0 \\ 1 & 0 & 0 \\ 0 & 0 & 0 \end{bmatrix}$	$\begin{bmatrix} 0 \\ 1 \\ -1 \end{bmatrix}$
4	$\begin{bmatrix} 1 & 1 & 0 & 0 & 1 & 0 & 1 & 0 & 0 & 0 \\ 0 & 1 & 1 & 0 & 0 & 0 & 0 & 0 & 0 & 0 \\ 1 & 0 & 1 & 0 & 0 & 1 & 0 & 1 & 0 & 0 \\ 1 & 0 & 1 & 0 & 0 & 0 & 0 & 0 & 0 & 0 \\ 1 & 0 & 0 & 0 & 0 & 0 & 0 & 1 & 0 & 0 \\ 0 & 0 & 0 & 1 & 0 & 0 & 0 & 1 & 0 & 0 \\ 0 & 0 & 1 & 0 & 0 & 0 & 0 & 0 & 0 & 0 \end{bmatrix}$	$\begin{bmatrix} 0.0143 \\ 0.0048 \\ -0.0048 \\ -0.0143 \end{bmatrix}$	$\begin{bmatrix} 0 & -\frac{1}{2} & 0 & 0 \\ \frac{1}{2} & 0 & 0 & 0 \\ 0 & 0 & 0 & -\frac{1}{3} \\ 0 & 0 & \frac{1}{3} & 0 \end{bmatrix}$	$\begin{bmatrix} 1 \\ 0 \\ 1 \\ 0 \end{bmatrix}$
5	$\begin{bmatrix} 0 & 1 & 0 & 0 & 0 & 0 & 0 \\ 0 & 0 & 0 & 0 & 1 & 1 & 0 \\ 0 & 0 & 0 & 1 & 0 & 0 & 0 \\ 2 & 0 & 0 & 0 & 1 & 1 & 0 \\ 1 & 0 & 1 & 0 & 0 & 0 & \frac{1}{2} \\ 0 & 0 & 1 & 1 & 0 & 0 & 0 \end{bmatrix}$	$\begin{bmatrix} -0.0238 \\ -0.0333 \\ -0.0429 \\ -0.0524 \end{bmatrix}$	$\begin{bmatrix} 0 & -2 \\ 2 & 0 \end{bmatrix}$	$\begin{bmatrix} 1 \\ 0 \end{bmatrix}$
6	$\begin{bmatrix} 0 & 1 & -1 & 0 & 0 & 0 & 0 & 0 & 0 \\ -1 & 0 & 1 & 0 & 0 & 0 & 0 & 0 & 0 \\ 0 & 1 & 0 & -1 & 0 & 0 & 0 & 0 & 0 \\ 1 & 0 & -2 & 0 & 0 & 1 & 0 & 1 & 0 \\ 0 & 0 & 0 & 0 & 0 & 0 & 1 & -2 & 0 \\ 0 & 0 & 0 & 1 & 0 & 0 & 0 & 0 & 2 \\ 0 & 0 & 0 & 0 & 1 & 0 & 0 & 0 & -1 \\ 1 & 0 & 0 & 0 & 0 & 0 & 0 & 0 & 0 \end{bmatrix}$	$\begin{bmatrix} -0.0619 \\ -0.0714 \\ -0.0810 \\ -0.0905 \\ -0.1000 \end{bmatrix}$	$\begin{bmatrix} 0 & 0 \\ 0 & 0 \end{bmatrix}$	$\begin{bmatrix} 1 \\ 1 \end{bmatrix}$

Table IV using the notation

$$\Sigma_i = \begin{bmatrix} A_i^p & B_i^p & B_i^w \\ C_i^p & & C_i^w \\ E_i^p & & \end{bmatrix}. \quad (101)$$

The disturbance models of each agent are also given in Table IV. The reference model is the same fourth-order oscillator of Example 2 in Section 3.6. The controller gain matrices K_i and L_i are computed also as described in Example 2, with the weights matrices given in Table V. The remaining gain matrices K_i^w and K_i^r are obtained from (38). Also included in Table V are the values selected for the parameters γ_i and σ_i of each agent. The initial conditions for $x_i^p(0)$ are given in Table IV, $x_i^c(0) = 0$ for $i \in \{1, \dots, N\}$, and $\zeta(0) = \hat{\zeta}(0) = g/\|g\|$ where $g \in \mathbb{R}^{mN}$ has entries

Table V. Weight matrices for controller design and parameters γ_i and σ_i associated with each agent.

i	$Q_p^i, R_p^i, Q_c^i, R_c^i$	σ_i, γ_i
1	$I_{n_p^1}, I_{n_u^1}, I_{n_c^1}, I_{n_y^1}$	0.95, 0.25
2	$I_{n_p^2}, I_{n_u^2}, 10I_{n_c^2}, I_{n_y^2}$	0.95, 0.5
3	$I_{n_p^3}, I_{n_u^3}, I_{n_c^3}, I_{n_y^3}$	0.95, 0.25
4	$I_{n_p^4}, I_{n_u^4}, 10I_{n_c^4}, I_{n_y^4}$	0.95, 0.25
5	$I_{n_p^5}, I_{n_u^5}, 100I_{n_c^5}, I_{n_y^5}$	0.95, 0.1
6	$I_{n_p^6}, I_{n_u^6}, 10I_{n_c^6}, I_{n_y^6}$	0.95, 0.1

Table VI. Statistics regarding the sequence of broadcast and sampling intervals ($\{b_{k+1}^i - b_k^i\}_{k \geq 0}$ and $\{s_{k+1}^i - s_k^i\}_{k \geq 0}$, respectively).

Agent i	Event detector	Observed minimum interval	Observed average interval	Observed maximum interval
1	broadcast	0.574 s	4.184 s	37.86 s
	sampling	0.598 ms	13.46 ms	266.3 ms
2	broadcast	0.393 s	3.232 s	19.50 s
	sampling	0.716 ms	15.73 ms	361.3 ms
3	broadcast	0.546 s	3.066 s	11.98 s
	sampling	1.058 ms	9.32 ms	375.4 ms
4	broadcast	0.369 s	1.769 s	10.27 s
	sampling	0.149 ms	6.08 ms	233.1 ms
5	broadcast	0.390 s	1.946 s	9.64 s
	sampling	0.046 ms	14.19 ms	262.4 ms
6	broadcast	0.505 s	2.652 s	12.84 s
	sampling	0.036 ms	16.42 ms	541.9 ms

$g_j = (2j - mN - 1)/(mN - 1)$ for $j \in \{1, \dots, mN\}$. The triggering parameters for the threshold function are $c_0 = 0.001$, $c_1 = 0.499$, and $\alpha = 0.25$. The communication graph \mathcal{G} is represented in Figure 8 (see Section A.1).

In Section 3.6, we have made the case in Example 3 that the asynchronous triggering mechanisms have implementation issues that result from a rather restrictive design procedure. For this reason, in the simulations performed in this section, we consider that the output and input event detectors operate synchronously as described in Section 3.3, for which the design procedure is less conservative. In this example, the (complete) sequence of sampling times of agent i is denoted by $\{s_k^i\}_{k \geq 0}$ and is defined as $\{s_k^i\}_{k \geq 0} = \{t_k^i\}_{k \geq 0} \cup \{b_k^i\}_{k \geq 0}$.

The trajectories of z_i for $i \in \{1, \dots, N\}$ are shown in Figure 7a, where it can be seen that the agents approximately synchronize their regulated outputs. This is supported by Figure 7b where the trajectory of $\max_i z_i - \min_i z_i$ is represented that measures the maximum misalignment possible among the regulated output of all pairs of agents. Assuming transients due to initial conditions have subsided after 50s, a numerical bound on the asymptotic misalignment is given by the maximum misalignment observed on the interval $[50, 100]$, which in this case is 3.879×10^{-2} . The sequences of sampling and broadcast intervals of agent $i = 4$ are shown in Figure 7c and Figure 7d, respectively. In Figure 7c, we have highlighted the sampling intervals that immediately precede a broadcast and that typically represent the lowest sampling intervals observed. In Table VI, we present, for each agent, the minimum, maximum, and average sampling and broadcast intervals observed in simulation.

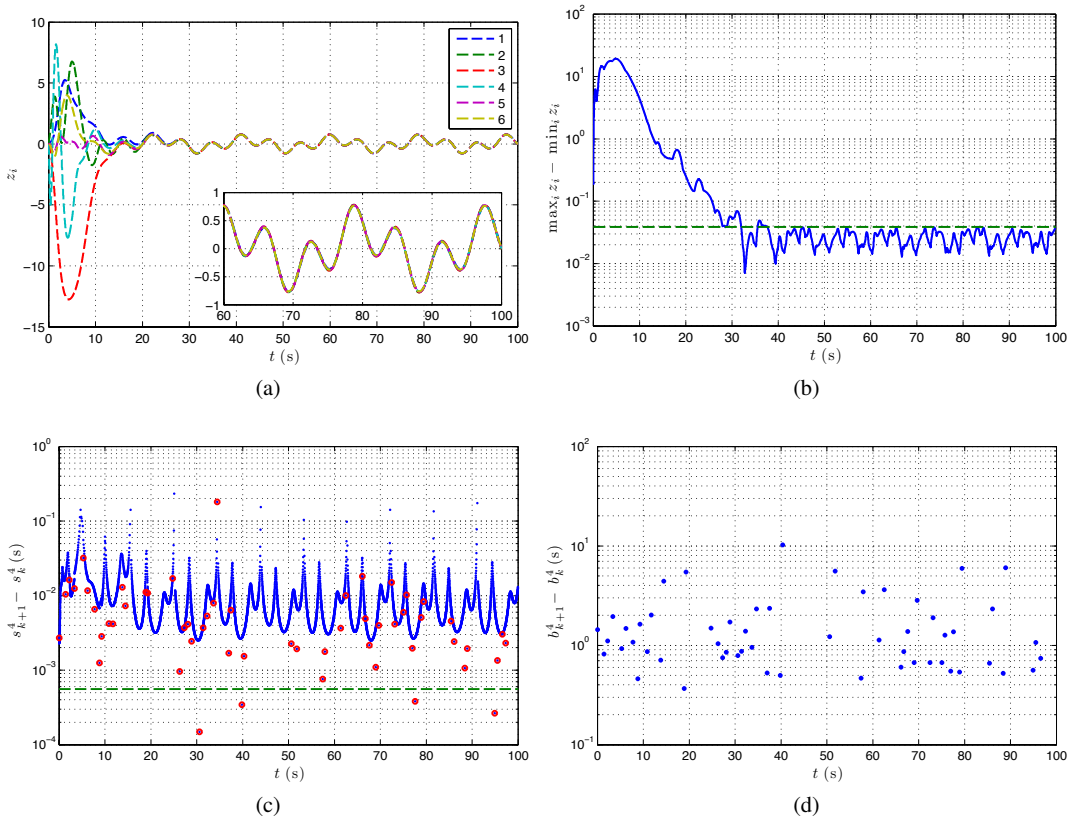


Figure 7. Simulation results for the event-triggered output synchronization controller with synchronous output and input event detectors. (a) Trajectory of z_i for each agent (on the southeast corner of the plot is a zoom on the last 40 s). (b) Trajectory of $\max_i z_i - \min_i z_i$ that measures the maximum misalignment possible among all pairs of agents. The dashed line represents the maximum misalignment observed on the interval $[50, 100]$, which is equal to 3.879×10^{-2} . (c) Sequence of sampling intervals of agent $i = 4$ where the dashed line represents the minimum sampling interval τ_{\min}^i . Highlighted in red are the sampling intervals that immediately precede a broadcast and that typically represent the lowest sampling intervals observed. (d) Sequence of broadcast intervals of agent $i = 4$.

5. CONCLUSION

In this paper we have proposed and analyzed a control architecture designed to achieve output synchronization of multi-agent systems using event-triggered output regulation controllers and event-triggered communication protocols.

We started by addressing the output regulation problem for a single agent where we considered two scenarios. In the first one, the output and input event detectors operated synchronously, while in second one they operated asynchronously. The event-triggered mechanisms proposed were inspired by the results in [35] on event-triggered output feedback stabilization. They employ simultaneously a time-triggered event condition and a state dependent one. It is shown that the proposed triggering methods achieve globally bounded tracking error for all bounded reference trajectories and all bounded disturbances. Examples are provided that illustrate the advantages and issues of the proposed triggering methods.

By merging the above mentioned results on output regulation with previous work on synchronization of reference generators, we proved that the regulated output of each agent converges to and remains in a neighborhood of a desired reference trajectory and that Zeno solutions are avoided. A multi-agent example was provided illustrating these facts.

Further results for nonlinear systems with quantization have been recently reported in [42], which reinforces the fact that event-triggered control techniques are becoming more wide spread.

ACKNOWLEDGEMENTS

This research was supported by the FCT (UID/EEA/50009/2013). The work of J. Almeida was funded by grant SFRH/BD/30605/2006 from Fundação para a Ciência e a Tecnologia (FCT).

A. AUXILIARY MATERIAL

A.1. Graph theory review

For an in-depth presentation of the subject, the reader is referred for example to [43] for a comprehensive textbook on the matter and to [2, 44, 45] for specific results regarding algebraic graph theory.

A (directed) graph $\mathcal{G} = \mathcal{G}(\mathcal{V}, \mathcal{E})$ consists of a finite set $\mathcal{V} = \{1, 2, \dots, N\}$ of N vertices and a finite set $\mathcal{E} \subseteq \mathcal{V} \times \mathcal{V}$ of m ordered pairs of vertices (i, j) named edges (in this paper, self-edges (i, i) are not allowed). An undirected graph is defined as a graph where $(i, j) \in \mathcal{E}$ if and only if $(j, i) \in \mathcal{E}$. If $(i, j) \in \mathcal{E}$, then we say that vertex i is an in-neighbor of vertex j and that j is an out-neighbor of vertex i . The set of in-neighbors and of out-neighbors of vertex i are defined as $\mathcal{N}_i^- = \{j \in \mathcal{V} : (j, i) \in \mathcal{E}\}$ and $\mathcal{N}_i^+ = \{j \in \mathcal{V} : (i, j) \in \mathcal{E}\}$, respectively. In an undirected graph, both sets are equal and simply referred to as neighbors of vertex i . A path in \mathcal{G} from vertex i to vertex j is a sequence of distinct edges of the form $\{(i, i_1), (i_1, i_2), \dots, (i_k, j)\}$. A vertex i is a root of a graph \mathcal{G} if there exists a path in \mathcal{G} from vertex i to every other vertex in \mathcal{G} . If \mathcal{G} has at least one root, we say that it is a rooted graph. If a graph \mathcal{G} is undirected and rooted, then it is said to be connected (in this case, all vertices are roots).

The adjacency matrix of a graph, denoted $\mathcal{A} = [a_{ij}] \in \mathbb{R}^{N \times N}$, is a square matrix with rows and columns indexed by the vertices and whose entries satisfy

$$a_{ij} = \begin{cases} 1, & (j, i) \in \mathcal{E}, \\ 0, & \text{otherwise.} \end{cases} \quad (102)$$

The in-degree matrix \mathcal{D} of a graph is a diagonal matrix where the i, i -entry is equal to the in-degree of vertex i (cardinality of \mathcal{N}_i^-). The Laplacian of a graph $\mathcal{L} = [l_{ij}] \in \mathbb{R}^{N \times N}$ is defined as

$$l_{ij} = \begin{cases} \sum_{k=1}^N a_{ik}, & i = j, \\ -a_{ij}, & \text{otherwise,} \end{cases} \quad (103)$$

that is equivalent to saying that $\mathcal{L} = \mathcal{D} - \mathcal{A}$. Next, we enumerate some important properties of the Laplacian.

Lemma 6

Let \mathcal{L} denote the Laplacian of a graph \mathcal{G} . Then, the following properties hold:

1. $\mathcal{L}\mathbf{1}_N = 0$;
2. $\exists \beta \in \mathbb{R}^N, \beta^\top \mathbf{1}_N = 1 : \beta^\top \mathcal{L} = 0$;
3. $\sigma(\mathcal{L}) = \{0, \lambda_2, \dots, \lambda_N\}$ with $\Re\{\lambda_i\} > 0$ for all non-zero eigenvalues;
4. \mathcal{G} is a rooted graph if and only if 0 is a simple eigenvalue of \mathcal{L} (this implies that $\Re\{\lambda_i\} > 0$ for $i = 2, \dots, N$);

Furthermore, if \mathcal{G} is undirected, then:

5. \mathcal{L} is symmetric and $\beta = \frac{1}{N}\mathbf{1}_N$;
6. $\lambda_i \geq 0$ for $i = 2, \dots, N$;
7. \mathcal{G} is connected if and only if 0 is a simple eigenvalue of \mathcal{L} (this implies that $\lambda_i > 0$ for $i = 2, \dots, N$).

To illustrate the aforementioned concepts, consider as an example the graph depicted in Figure 8 with vertex set $\mathcal{V} = \{1, 2, 3, 4, 5, 6\}$ and edge set $\mathcal{E} = \{(1, 3); (2, 1); (2, 4); (3, 2); (3, 5); (4, 5); (5, 6); (6, 4)\}$. The adjacency and Laplacian matrices associated with the graph are

$$\mathcal{A} = \begin{bmatrix} 0 & 1 & 0 & 0 & 0 & 0 \\ 0 & 0 & 1 & 0 & 0 & 0 \\ 1 & 0 & 0 & 0 & 0 & 0 \\ 0 & 1 & 0 & 0 & 0 & 1 \\ 0 & 0 & 1 & 1 & 0 & 0 \\ 0 & 0 & 0 & 0 & 1 & 0 \end{bmatrix} \quad \text{and} \quad \mathcal{L} = \begin{bmatrix} 1 & -1 & 0 & 0 & 0 & 0 \\ 0 & 1 & -1 & 0 & 0 & 0 \\ -1 & 0 & 1 & 0 & 0 & 0 \\ 0 & -1 & 0 & 2 & 0 & -1 \\ 0 & 0 & -1 & 0 & 2 & 0 \\ 0 & 0 & 0 & 0 & -1 & 1 \end{bmatrix}, \quad (104)$$

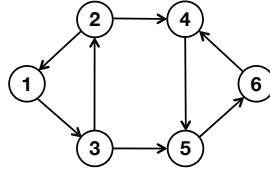


Figure 8. A graph with 6 vertices and 8 edges. Consider, for example, vertex 5. Its set of in-neighbors is $\mathcal{N}_5^- = \{3, 4\}$ and its set of out-neighbors is $\mathcal{N}_5^+ = \{6\}$. Vertices 1, 2, and 3 are all roots because there exists a directed path from them to every other vertex in the graph.

respectively. The spectrum of the Laplacian is $\sigma(\mathcal{L}) = \{0, 0.5344, 1.5000 \pm i0.8660, 2.2328 \pm i0.7926\}$ and $\beta = (\frac{1}{3}, \frac{1}{3}, \frac{1}{3}, 0, 0, 0)$.

A.2. Linear impulsive systems

Impulsive systems combine continuous evolution (typically modeled by ordinary differential equations) with instantaneous state jumps (also referred to as resets or impulses). Stability properties of such systems have been extensively investigated in the literature (see, e.g., [46, 47]).

We define a linear impulsive system as a system with state $x \in \mathbb{R}^n$ and initial state $x(t_0) = x_0$, for some initial time $t_0 \in \mathbb{R}$, that satisfies, for all $t \geq t_0$,

$$\begin{cases} \dot{x}(t) = Ax(t), & t \in [t_k, t_{k+1}), k \in \{0, 1, \dots\}, \\ x(t) = Jx^-(t), & t = t_k, k \in \{1, 2, \dots\}, \end{cases} \quad (105a)$$

$$\quad (105b)$$

where $\{t_k\}_{k \geq 0} = \{t_0, t_1, t_2, \dots\}$ is a strictly increasing sequence of impulse times in (t_0, ∞) .^{‡‡} The sequence of impulse times is assumed to be either finite ($\{t_0, t_1, \dots, t_K\}$) or infinite and unbounded ($\lim_{k \rightarrow \infty} t_k = +\infty$). In particular, we exclude the possibility of $\{t_k\}_{k \geq 0}$ having any accumulation point, often referred to as Zeno solutions. An accumulation point of a sequence $\{t_k\}_{k \geq 0}$ with elements in \mathbb{R} is a point $t^* \in \mathbb{R}$ if for every neighborhood \mathcal{U} of t^* , the set $\mathcal{U} \cap \{t_k\}_{k \geq 0}$ contains infinitely many points. The following facts are used to excluded the occurrence of sequences with such points.

1. A sequence $\{t_k\}_{k \geq 0}$ does not have any accumulation points if there exists $\tau_{\min} > 0$ such that $t_{k+1} - t_k \geq \tau_{\min}$ for all $k \geq 0$.
2. A sequence obtained from a finite union of sequences without accumulation points, does not have accumulation points.

A.3. Definition of ISS and ISpS

The following definitions are borrowed from [48, Chapter 4] and [49]. Consider the system

$$\dot{x} = f(t, x, u) \quad (106)$$

where $f : [0, \infty) \times \mathbb{R}^n \times \mathbb{R}^m \rightarrow \mathbb{R}^n$ is piecewise continuous in t and locally Lipschitz in x and u . The input $u(t)$ is a piecewise continuous, bounded function of t for all $t \geq 0$. A continuous function $\alpha : [0, \infty) \rightarrow [0, \infty)$ is said to belong to class \mathcal{K}_∞ if it is strictly increasing, $\alpha(0) = 0$, and $\alpha(r) \rightarrow \infty$ as $r \rightarrow \infty$. A continuous function $\beta : [0, \infty) \times [0, \infty) \rightarrow [0, \infty)$ is said to belong to class \mathcal{KL} if, for fixed s , the mapping $\beta(r, s)$ belongs to class \mathcal{K}_∞ with respect to r and, for fixed r , the mapping $\beta(r, s)$ is decreasing with respect to s and $\beta(r, s) \rightarrow 0$ as $s \rightarrow \infty$.

The system (106) is said to be *input-to-state stable* (ISS) if there exist a class \mathcal{KL} function β and a class \mathcal{K}_∞ function ρ such that for any initial state $x(t_0)$ and any bounded input $u(t)$, the solution $x(t)$ exists for all $t \geq t_0$ and satisfies

$$\|x(t)\| \leq \beta(\|x(t_0)\|, t - t_0) + \rho \left(\sup_{t_0 \leq \tau \leq t} \|u(\tau)\| \right). \quad (107)$$

The system (106) is said to be *input-to-state practically stable* (ISpS) if there exist a class \mathcal{KL} function β , a class \mathcal{K}_∞ function ρ , and a constant $c \geq 0$ such that for any initial state $x(t_0)$ and any bounded input $u(t)$,

^{‡‡}We include t_0 in the sequence of impulse times to simplify the notation.

the solution $x(t)$ exists for all $t \geq t_0$ and satisfies

$$\|x(t)\| \leq \beta(\|x(t_0)\|, t - t_0) + \rho \left(\sup_{t_0 \leq \tau \leq t} \|u(\tau)\| \right) + c. \quad (108)$$

The difference between ISS and ISpS is that the latter allows a non-zero constant c .

A.4. Schur complement

The following is adapted from [50, Appendix A.5.5]. Let $x = (x_1, x_2)$ where $x_1 \in \mathbb{R}^{n_1}$ and $x_2 \in \mathbb{R}^{n_2}$. Given a symmetric matrix $U \in \mathbb{R}^{(n_1+n_2) \times (n_1+n_2)}$, let $U = \begin{bmatrix} A & B \\ * & C \end{bmatrix}$ be a partition compatible with the partition of x . If $A \prec 0$, then

$$x^\top U x \leq \max_{x_1 \in \mathbb{R}^{n_1}} x^\top U x = x_2^\top (C - B^\top A^{-1} B) x_2, \quad (109)$$

where $C - B^\top A^{-1} B$ is the Schur complement of A . If $A \succ 0$, then $x^\top U x \geq x_2^\top (C - B^\top A^{-1} B) x_2$.

B. PROOFS

B.1. Proof of Lemma 1

From (44), we have that \tilde{x} and ψ are continuous for all $t \geq 0$. Since (53) holds for all $t \geq 0$, \dot{V} given in (51) satisfies (54) for all $t \geq 0$.

Using (48) in (54), we obtain that

$$\dot{V}(\tilde{x}(t)) \leq -\lambda V(\tilde{x}(t)) + \gamma^2 \|\psi(t)\|^2, \quad (110)$$

for all $t \geq 0$. Integrating (110) from 0 to t yields

$$V(\tilde{x}(t)) \leq e^{-\lambda t} V(\tilde{x}(0)) + \int_0^t \gamma^2 e^{-\lambda(t-s)} \|\psi(s)\|^2 ds \quad (111)$$

$$\leq e^{-\lambda t} V(\tilde{x}(0)) + \gamma^2 \|\psi\|_{\mathcal{L}_\infty}^2 \int_0^t e^{-\lambda(t-s)} ds \quad (112)$$

$$\leq e^{-\lambda t} V(\tilde{x}(0)) + \frac{\gamma^2}{\lambda} \|\psi\|_{\mathcal{L}_\infty}^2. \quad (113)$$

Using the fact that $\lambda_{\min}(P) \|\tilde{x}\|^2 \leq V(\tilde{x}) \leq \lambda_{\max}(P) \|\tilde{x}\|^2$, we have that

$$\|\tilde{x}(t)\|^2 \leq e^{-\lambda t} \frac{\lambda_{\max}(P)}{\lambda_{\min}(P)} \|\tilde{x}(0)\|^2 + \frac{\gamma^2}{\lambda_{\min}(P)\lambda} \|\psi\|_{\mathcal{L}_\infty}^2, \quad (114)$$

from which we derive that

$$\|\tilde{x}(t)\| \leq e^{-\frac{1}{2}\lambda t} \sqrt{\frac{\lambda_{\max}(P)}{\lambda_{\min}(P)}} \|\tilde{x}(0)\| + \frac{\gamma}{\sqrt{\lambda_{\min}(P)\lambda}} \|\psi\|_{\mathcal{L}_\infty} \quad (115)$$

$$= \beta(t, \|\tilde{x}(0)\|) + \rho_0 (\|\psi\|_{\mathcal{L}_\infty}). \quad (116)$$

This shows that (46) is input-to-state stable (ISS) from ψ to \tilde{x} , thus proving 1). Since by assumption Zeno solutions are avoided, we have that the limit in (55) exists. Then, 2) is obtained by using (35d) and (113), yielding

$$\lim_{t \rightarrow +\infty} \|e_r(t)\| \stackrel{(35d)}{=} \lim_{t \rightarrow +\infty} \|E_p(x_p(t) - \Pi_r x_r(t))\| \quad (117)$$

$$= \lim_{t \rightarrow +\infty} \|\bar{E}\tilde{x}(t)\| \quad (118)$$

$$\leq \lim_{t \rightarrow +\infty} \left\| \bar{E}P^{-1/2} \right\| \sqrt{V(\tilde{x}(t))} \quad (119)$$

$$\stackrel{(113)}{\leq} \frac{\gamma}{\sqrt{\lambda}} \left\| \bar{E}P^{-1/2} \right\| \|\psi\|_{\mathcal{L}_\infty}, \quad (120)$$

where we used the fact that $\tilde{x}^\top \bar{E}^\top \bar{E} \tilde{x} \leq \lambda_{\max}(P^{-\frac{1}{2}} \bar{E}^\top \bar{E} P^{-\frac{1}{2}}) \tilde{x}^\top P \tilde{x}$.

B.2. Proof of Lemma 2

For all $k \geq 0$, we have that

$$\xi^\top(t_k)M_0\xi(t_k) = \begin{bmatrix} \tilde{x}(t_k) \\ \psi(t_k) \end{bmatrix}^\top \begin{bmatrix} I \\ 0 \end{bmatrix}^\top M_0 \begin{bmatrix} I \\ 0 \end{bmatrix} \begin{bmatrix} \tilde{x}(t_k) \\ \psi(t_k) \end{bmatrix} \quad (121)$$

$$= \begin{bmatrix} \tilde{x}(t_k) \\ \psi(t_k) \end{bmatrix}^\top \begin{bmatrix} -\sigma Q & 0 \\ 0 & -\gamma^2 I_{n_\psi} \end{bmatrix} \begin{bmatrix} \tilde{x}(t_k) \\ \psi(t_k) \end{bmatrix} < 0, \text{ for all } \begin{bmatrix} \tilde{x}(t_k) \\ \psi(t_k) \end{bmatrix} \neq 0. \quad (122)$$

This shows that when $\tilde{\mu}$ is reset to zero, (53) is always satisfied. Suppose (53) holds for all $t \in [0, t_k]$. Then, (122) and the fact that $\xi(t)$ is a continuous function in t imply there exists $t^* > t_k$ such that $\xi(t^*)^\top M_0\xi(t^*) = 0$ and $\xi(t)^\top M_0\xi(t) \leq 0$ for all $t \in [t_k, t^*)$. From (56), we see that t_{k+1} is the smallest possible t^* , which implies that $\xi(t)^\top M_0\xi(t) \leq 0$ for all $t \in [0, t_{k+1}]$. Proceeding by induction in k , we conclude that (53) holds for all $t \in [0, \lim_{k \rightarrow \infty} t_k]$. We show that $\lim_{k \rightarrow \infty} t_k = +\infty$ by proving the existence of τ_{\min} .

Let k be fixed. Then, solving (44) in t yields that, for all $t \geq t_k$,

$$\xi(t) = e^{\bar{A}(t-t_k)}\xi(t_k) = e^{\bar{A}(t-t_k)} \begin{bmatrix} I \\ 0 \end{bmatrix} \begin{bmatrix} \tilde{x}(t_k) \\ \psi(t_k) \end{bmatrix}. \quad (123)$$

Thus, we have that, for all $t \geq t_k$,

$$\xi^\top(t)M_0\xi(t) = \begin{bmatrix} \tilde{x}(t_k) \\ \psi(t_k) \end{bmatrix}^\top \begin{bmatrix} I \\ 0 \end{bmatrix}^\top e^{\bar{A}^\top(t-t_k)} M_0 e^{\bar{A}(t-t_k)} \begin{bmatrix} I \\ 0 \end{bmatrix} \begin{bmatrix} \tilde{x}(t_k) \\ \psi(t_k) \end{bmatrix} \quad (124)$$

$$\leq h(t-t_k) \left\| \begin{bmatrix} \tilde{x}(t_k) \\ \psi(t_k) \end{bmatrix} \right\|^2 \quad (125)$$

where the function h is defined in (58). Since h is a continuous function of s and

$$h(0) = \lambda_{\max} \left\{ \begin{bmatrix} -\sigma Q & 0 \\ 0 & -\gamma^2 I_{n_\psi} \end{bmatrix} \right\} = -\min \left\{ \sigma \lambda_{\min}(Q), \gamma^2 \right\} < 0, \quad (126)$$

there exists $\tau_{\min} > 0$ such that $h(s) < 0$ for $s \in [0, \tau_{\min})$. If we take $t^* = t_k + \tau_{\min}$, then $\xi^\top(t^*)M_0\xi(t^*) < 0$. Thus, $t_{k+1} > t^* \Leftrightarrow \tau_k > \tau_{\min}$ that is satisfied for all $k \geq 0$ because the existence of τ_{\min} is independent of k .

Finally, (57) implies that $\tau_{\min} \leq \tau_{\min}^*$ where τ_{\min}^* is attainable because there exists an initial condition such that the sampling interval is precisely τ_{\min}^* , namely any initial condition that belongs to the kernel of

$$\begin{bmatrix} I \\ 0 \end{bmatrix}^\top e^{\bar{A}^\top \tau_{\min}^*} M_0 e^{\bar{A} \tau_{\min}^*} \begin{bmatrix} I \\ 0 \end{bmatrix}. \quad (127)$$

B.3. Proof of Lemma 3

The first event condition in (59), guarantees that $\xi^\top(t)M_0\xi(t) \leq 0$ for all $t \in [t_k, t_k + \tau_{\min}]$. At $t = t_k + \tau_{\min}$, one of two situations may happen.

1. If $\phi^\top(t)M\phi(t) \geq 0$, then $t_{k+1} = t_k + \tau_{\min}$.
2. Otherwise, there exists $t_{k+1} > t_k + \tau_{\min}$ such that $\phi^\top(t)M\phi(t) \leq 0$ for all $t \in [t_k + \tau_{\min}, t_{k+1})$. Because of (60), we have that

$$\xi^\top(t)M_0\xi(t) \leq \phi^\top(t)M\phi(t) \leq 0 \quad (128)$$

for all $t \in [t_k + \tau_{\min}, t_{k+1})$.

In any case, we have that $\xi^\top(t)M_0\xi(t) \leq 0$ for all $t \in [t_k, t_{k+1})$. Note that, by definition, $\tau_k \geq \tau_{\min}$ and thus $\lim_{k \rightarrow \infty} t_k = +\infty$. Therefore, $\xi^\top(t)M_0\xi(t) \leq 0$ for all $t \geq 0$.

B.4. Sub-matrix of \widehat{M}_0 is negative definite

To check that in (66) the Schur complement technique may be applied to the matrix \widehat{M}_0 , we have to show that the appropriate sub-matrix of \widehat{M}_0 is negative definite. First, note that the matrix T in (61) and \widehat{Z}_c in (63) are invertible. Therefore, $T\widehat{Z}_c$ is also invertible and may be written as

$$T\widehat{Z}_c = \begin{bmatrix} T_1\widehat{Z}_1 & 0 \\ 0 & I_{n_\mu} \end{bmatrix}. \quad (129)$$

Using this decomposition, we may write \widehat{M}_0 as

$$\widehat{M}_0 = \begin{bmatrix} T_1\widehat{Z}_1 & 0 \\ 0 & I_{n_\mu} \end{bmatrix}^\top M_0 \begin{bmatrix} T_1\widehat{Z}_1 & 0 \\ 0 & I_{n_\mu} \end{bmatrix} = \begin{bmatrix} -\widehat{Q} & \widehat{G} \\ * & 0_{n_\mu} \end{bmatrix} \quad (130)$$

where $\widehat{Q} \succ 0$. This shows that the sub-matrix of \widehat{M}_0 associated with x_u is negative-definite and thus we may apply the Schur complement technique to \widehat{M}_0 to obtain M .

B.5. Proof of Theorem 3

From the definition of the triggering mechanism in (59), $\{t_k\}_{k \geq 0}$ satisfies $\tau_k \geq \tau_{\min} > 0$ for all $k \geq 0$, which implies 1) as stated in Section A.2. Lemma 3 guarantees that (53) holds for all $t \geq 0$. Therefore, by Lemma 1, 2) and 3) hold.

B.6. Proof of Lemma 4

The proof follows along the same arguments used in Lemma 1 of [35]. For $t \in [t_k, t_{k+1})$, (44) implies that

$$\dot{\hat{\xi}} = F\hat{\xi} + \begin{bmatrix} G_y \\ 0 \end{bmatrix} \tilde{y} + \begin{bmatrix} G_u \\ 0 \end{bmatrix} \tilde{u}. \quad (131)$$

Note that $\tilde{y} = -H_y\hat{\xi}$ and $\tilde{u} = -H_u\hat{\xi}$. We want to find $\tau_{\min}^y > 0$ such that

$$\nu_y(t) = \frac{\|\tilde{y}(t)\|}{\|\hat{\xi}(t)\|} \leq w_y \quad (132)$$

holds for all $t \in [t_k^y, t_k^y + \tau_{\min}^y)$. To accomplish this we need a bound on the evolution of ν_y . We have that

$$\dot{\nu}_y = \frac{d}{dt} \left(\frac{\tilde{y}^\top \tilde{y}}{\hat{\xi}^\top \hat{\xi}} \right)^{\frac{1}{2}} \quad (133)$$

$$= \left(\frac{\hat{\xi}^\top \hat{\xi}}{\tilde{y}^\top \tilde{y}} \right)^{\frac{1}{2}} \frac{(\tilde{y}^\top \dot{\tilde{y}})(\hat{\xi}^\top \hat{\xi}) - (\tilde{y}^\top \tilde{y})(\hat{\xi}^\top \dot{\hat{\xi}})}{(\hat{\xi}^\top \hat{\xi})^2} \quad (134)$$

$$\leq \frac{\|\hat{\xi}\|}{\|\tilde{y}\|} \left(\frac{\|H_y\| \|\tilde{y}\| \|\hat{\xi}\|^2 + \|\tilde{y}\|^2 \|\hat{\xi}\|}{\|\hat{\xi}\|^4} \right) \|\dot{\hat{\xi}}\| \quad (135)$$

$$\leq \left(\|H_y\| + \frac{\|\tilde{y}\|}{\|\hat{\xi}\|} \right) \frac{\|F\| \|\hat{\xi}\| + \|G_y\| \|\tilde{y}\| + \|G_u\| \|\tilde{u}\|}{\|\hat{\xi}\|} \quad (136)$$

$$= (\|H_y\| + \nu_y)(\|F\| + \|G_y\| \nu_y + \|G_u\| \nu_u) \quad (137)$$

where $\nu_u = \|\tilde{u}\|/\|\hat{\xi}\|$. By assumption, we have that $\{t_k^u\}_{k \geq 0}$ is such that $\nu_u(t) \leq w_u$ holds for all $t \geq 0$. Therefore,

$$\dot{\nu}_y \leq (\|H_y\| + \nu_y)(\|F\| + \|G_y\| \nu_y + \|G_u\| w_u) \quad (138)$$

and $\nu_y(t_k^y) = 0$. Using the comparison principle (see, e.g., [48]), we conclude that the solution ν of (74) with $a = \|F\| + \|G_u\| w_u$, $b = \|G_y\|$, and $c = \|H_y\|$ satisfies $\nu_y(t_k^y + s) \leq \nu(s)$ for all $s \geq 0$. Therefore, the time it takes for ν_y to grow from $\nu_y(t_k^y) = 0$ to w_y is greater than or equal to τ_{\min}^y . The same approach may be applied to ν_u to arrive at the same conclusion regarding τ_{\min}^u .

B.7. Proof of Lemma 5

Suppose $\|\tilde{u}(t)\| - w_u \|\hat{\xi}(t)\| \leq 0$ for all $t \geq 0$. Then, the first event condition in (79a) guarantees that $\|\tilde{y}(t)\| - w_y \|\hat{\xi}(t)\| \leq 0$ for all $t \in [t_k^y, t_k^y + \tau_{\min}^y]$. At $t = t_k^y + \tau_{\min}^y$, one of two situations may happen.

1. If $\phi_y^\top(t_k^y + \tau_{\min}^y) M_y \phi_y(t_k^y + \tau_{\min}^y) \geq 0$, then $t_{k+1}^y = t_k^y + \tau_{\min}^y$.
2. Otherwise, since $\phi_y(t)$ is a continuous function for $t \geq t_k^y$, there exists $t_{k+1}^y > t_k^y + \tau_{\min}^y$ such that $\phi_y^\top(t_{k+1}^y) M_y \phi_y(t_{k+1}^y) = 0$ and $\phi_y^\top(t) M_y \phi_y(t) < 0$ for all $t \in [t_k^y + \tau_{\min}^y, t_{k+1}^y]$. From (77a) and (78), we conclude that

$$\phi_y^\top(t) M_y \phi_y(t) \leq 0 \Rightarrow \|\tilde{y}(t)\| - w_y \|\hat{\xi}(t)\| \leq 0 \quad (139)$$

for all $t \in [t_k^y + \tau_{\min}^y, t_{k+1}^y]$.

In any case, we have that $\|\tilde{y}(t)\| - w_y \|\hat{\xi}(t)\| \leq 0$ for all $t \in [t_k^y, t_{k+1}^y]$. Note that, by definition, $\tau_k^y \geq \tau_{\min}^y$ and thus $\lim_{k \rightarrow \infty} t_k^y = +\infty$. Therefore, $\|\tilde{y}(t)\| - w_y \|\hat{\xi}(t)\| \leq 0$ for all $t \geq 0$. Proceeding in the same manner for $\{t_k^u\}_{k \geq 0}$, leads to the conclusion that $\|\tilde{u}(t)\| - w_u \|\hat{\xi}(t)\| \leq 0$ for all $t \geq 0$, which confirms our initial assumption.

Therefore, (73) holds for all $t \geq 0$ and from the chain of implications (73) \Rightarrow (70) \Rightarrow (53), it follows that (53) holds for all $t \geq 0$.

B.8. Proof of Theorem 4

From the definition of the triggering mechanisms in (79), we have that $\{t_k^y\}_{k \geq 0}$ and $\{t_k^u\}_{k \geq 0}$ satisfy $\tau_k^y \geq \tau_{\min}^y > 0$ and $\tau_k^u \geq \tau_{\min}^u > 0$ for all $k \geq 0$, respectively. Then, $\{t_k\}_{k \geq 0} = \{t_k^y\}_{k \geq 0} \cup \{t_k^u\}_{k \geq 0}$ does not have accumulation points (see Section A.2), which proves 1). Lemma 5 implies that (54) holds for all $t \geq 0$. Therefore, by Lemma 1, 2) and 3) hold.

B.9. Proof of Theorem 5

Consider the signal $\zeta_0(t)$ defined in (3). Using the initial condition $\zeta_0(0) = (\beta^\top \otimes I_m) \zeta(0)$ and solving (3a) in t , yields $\zeta_0(t) = e^{A_r t} (\beta^\top \otimes I_m) \zeta(0)$ for all $t \geq 0$. Therefore, (100) may be rewritten as $\|z_i - E_r \zeta_0\| \leq d$. Next, note that

$$z_i - E_r \zeta_0 = E_i^p \left(\tilde{x}_i^p + \Pi_{r,i} \hat{\zeta}_i + \Pi_i^w w_i \right) - E_r \zeta_0 \quad (140)$$

$$= E_i^p \tilde{x}_{r,i} + E_r \left(\hat{\zeta}_i - \zeta_0 \right) \quad (141)$$

$$= \bar{E}_i \tilde{x}_i + E_r \left(\hat{\zeta}_i - \zeta_0 \right), \quad (142)$$

where $\bar{E}_i = [E_i^p \quad 0] \in \mathbb{R}^{r \times (n_i^p + n_i^c)}$. We will show that each of the terms in (142) is bounded, thereby showing that there exists $d > 0$ such that (100) holds.

First, note that $\hat{\zeta}_i - \zeta_0$ may be written as $\hat{\zeta}_i - \zeta_0 = (\zeta_i - \zeta_0) + (\hat{\zeta}_i - \zeta_i)$. The signal $\zeta_i - \zeta_0$ is bounded because it satisfies $\|\zeta_i - \zeta_0\| \leq \|\delta\| \leq \bar{\delta}$, which follows from (24). The signal $\hat{\zeta}_i - \zeta_i$ is equal to e_i that is bounded by the definition of the triggering condition in (22). Therefore, $\hat{\zeta}_i - \zeta_0$ is bounded.

Regarding the term $\bar{E}_i \tilde{x}_i$, by Theorem 4, we have that \tilde{x}_i is ISS with respect to w_i and $\hat{\zeta}_i$. The disturbance w_i is bounded since A_i^w is skew-symmetric by Assumption 1. The signal $\hat{\zeta}_i$ is bounded because $\hat{\zeta}_i - \zeta_0$ is bounded (as shown above) and ζ_0 is bounded (since A_i^r is skew-symmetric by Assumption 1). We conclude that \tilde{x}_i is bounded that, together with the previous argument, proves that (100) holds.

Next, we show that the closed-loop system does not exhibit Zeno solutions. Note that $\{t_k^{y,i}\}_{k \geq 0}$, $\{t_k^{u,i}\}_{k \geq 0}$, and $\{b_k^i\}_{k \geq 0}$ to not have accumulation points because they satisfy $\tau_k^{y,i} \geq \tau_{\min}^y$, $\tau_k^{u,i} \geq \tau_{\min}^u$, and $b_{k+1}^i - b_k^i \geq \theta_{\min}$, respectively. Let $\{s_k^i\}_{k \geq 0} = \{b_k^i\}_{k \geq 0} \cup \{t_k^{y,i}\}_{k \geq 0} \cup \{t_k^{u,i}\}_{k \geq 0}$ denote the sequence of all event times of agent i . Then, the sequence of all event times occurring in the closed-loop system is defined as

$$\{s_k\}_{k \geq 0} = \bigcup_{i=1}^N \{s_k^i\}_{k \geq 0} = \bigcup_{i=1}^N \{b_k^i\}_{k \geq 0} \cup \{t_k^{y,i}\}_{k \geq 0} \cup \{t_k^{u,i}\}_{k \geq 0}, \quad (143)$$

which does not have accumulation points since it is the finite union of sequences without accumulation points.

REFERENCES

1. Ren W, Beard RW. *Distributed Consensus in Multi-vehicle Cooperative Control*. Communications and Control Engineering, Springer-Verlag: London, 2008.
2. Tsitsiklis JN, Bertsekas DP. *Parallel and Distributed Computation: Numerical Methods*. Prentice-Hall: New Jersey, USA, 1989.
3. Olfati-Saber R, Murray RM. Consensus problems in networks of agents with switching topology and time-delays. *IEEE Transactions on Automatic Control* Sep 2004; **49**(9):1520–1533, doi:10.1109/TAC.2004.834113.
4. Moreau L. Stability of multiagent systems with time-dependent communication links. *IEEE Transactions on Automatic Control* Feb 2005; **50**(2):169–182, doi:10.1109/TAC.2004.841888.
5. Münz U, Papachristodoulou A, Allgöwer F. Consensus reaching in multi-agent packet-switched networks with non-linear coupling. *International Journal of Control* May 2009; **82**(5):953–969, doi:10.1080/00207170802398018.
6. Sarlette A, Sepulchre R. Consensus optimization on manifolds. *SIAM Journal of Control and Optimization* Feb 2009; **48**(1):56–76, doi:10.1137/060673400.
7. Liu K, Ji Z, Xie G, Wang L. Consensus for heterogeneous multi-agent systems under fixed and switching topologies. *Journal of the Franklin Institute* Sep 2015; **352**(9):3670–3683, doi:10.1016/j.jfranklin.2015.03.009.
8. Fax J, Murray R. Information flow and cooperative control of vehicle formations. *IEEE Transactions on Automatic Control* Sep 2004; **49**(9):1465–1476, doi:10.1109/TAC.2004.834433.
9. Scardovi L, Sepulchre R. Synchronization in networks of identical linear systems. *Automatica* Nov 2009; **45**(11):2557–2562, doi:10.1016/j.automatica.2009.07.006.
10. Wieland P, Sepulchre R, Allgöwer F. An internal model principle is necessary and sufficient for linear output synchronization. *Automatica* May 2011; **47**(5):1068–1074, doi:10.1016/j.automatica.2011.01.081.
11. Zhu L, Chen Z, Middleton R. A general framework for robust output synchronization of heterogeneous nonlinear networked systems. *IEEE Transactions on Automatic Control* Oct 2015; doi:10.1109/TAC.2015.2492141. (in press).
12. Šiljak DD. *Decentralized control of complex systems*. Academic Press: San Diego, CA, USA, 1991.
13. Knobloch HW, Isidori A, Flockerzi D. *Topics in control theory*. Birkhäuser Verlag: Basel, 1993.
14. Saberi A, Stoorvogel AA, Sannuti P. *Control of linear systems with regulation and input constraints*. Springer: London, 2000.
15. Tabuada P. Event-triggered real-time scheduling of stabilizing control tasks. *IEEE Transactions on Automatic Control* Sep 2007; **52**(9):1680–1685, doi:10.1109/TAC.2007.904277.
16. Åström KJ. Event based control. *Analysis and Design of Nonlinear Control Systems*, Astolfi A, Marconi L (eds.). Springer Berlin Heidelberg, 2008; 127–147.
17. Heemels WPMH, Sandee JH, van den Bosch PPI. Analysis of event-driven controllers for linear systems. *International Journal of Control* Apr 2008; **81**(4):571–590, doi:10.1080/00207170701506919.
18. Lunze J, Lehmann D. A state-feedback approach to event-based control. *Automatica* Jan 2010; **46**(1):211–215.
19. Donkers MCF, Heemels WPMH. Output-based event-triggered control with guaranteed \mathcal{L}_∞ -gain and improved and decentralized event-triggering. *IEEE Transactions on Automatic Control* Jun 2012; **57**(6):1362–1376, doi:10.1109/TAC.2011.2174696.
20. Hu S, Yue D. \mathcal{L}_2 -gain analysis of event-triggered networked control systems: a discontinuous Lyapunov functional approach. *Int. Journal of Robust and Nonlinear Control* 2012; doi:10.1002/rnc.2815.
21. Jetto L, Orsini V. A new event-driven output-based discrete-time control for the sporadic MIMO tracking problem. *Int. Journal of Robust and Nonlinear Control* 2012; doi:10.1002/rnc.2921.
22. Heemels WPMH, Donkers MCF, Teel AR. Periodic event-triggered control for linear systems. *IEEE Transactions on Automatic Control* Apr 2013; **58**(4):847–861, doi:10.1109/TAC.2012.2220443.
23. Wang X, Lemmon MD. Event-triggering in distributed networked control systems. *IEEE Transactions on Automatic Control* Mar 2011; **56**(3):586–601, doi:10.1109/TAC.2010.2057951.
24. De Persis C, Sailer R, Wirth F. On a small-gain approach to distributed event-triggered control. *Preprints of the 18th IFAC World Congress*, Milano, Italy, 2011; 2401–2406, doi:10.3182/20110828-6-IT-1002.02057.
25. Wang X, Sun Y, Hovakimyan N. Asynchronous task execution in networked control systems using decentralized event-triggering. *Systems & Control Letters* Sep 2012; **61**(9):936–944, doi:10.1016/j.sysconle.2012.05.010.
26. Velasco M, Martí P, Fuentès JM. The self triggered task model for real-time control systems. *Proc. of the 24th IEEE Real-Time Systems Symp. (work in progress session)*, Cancun, Mexico, 2003; 67–70.
27. Wang X, Lemmon MD. Self-triggered feedback control systems with finite-gain \mathcal{L}_2 stability. *IEEE Transactions on Automatic Control* Mar 2009; **54**(3):452–467, doi:10.1109/TAC.2009.2012973.
28. Anta A, Tabuada P. To sample or not to sample: Self-triggered control for nonlinear systems. *IEEE Transactions on Automatic Control* Sep 2010; **55**(9):2030–2042, doi:10.1109/TAC.2010.2042980.
29. Mazo Jr M, Anta A, Tabuada P. An ISS self-triggered implementation of linear controllers. *Automatica* Aug 2010; **46**(8):1310–1314, doi:10.1016/j.automatica.2010.05.009.
30. Almeida J, Silvestre C, Pascoal AM. Self-triggered state feedback control of linear plants under bounded disturbances. *Int. Journal of Robust and Nonlinear Control* 2014; doi:10.1002/rnc.3138.
31. Dimarogonas DV, Frazzoli E, Johansson KH. Distributed event-triggered control for multi-agent systems. *IEEE Transactions on Automatic Control* May 2012; **57**(5):1291–1297, doi:10.1109/TAC.2011.2174666.
32. Seyboth GS, Dimarogonas DV, Johansson KH. Event-based broadcasting for multi-agent average consensus. *Automatica* Jan 2013; **49**(1):245–252, doi:10.1016/j.automatica.2012.08.042.

33. Guo G, Ding L, Han QL. A distributed event-triggered transmission strategy for sampled-data consensus of multi-agent systems. *Automatica* May 2014; **50**(5):1489–1496, doi:10.1016/j.automatica.2014.03.017.
34. Almeida J, Silvestre C, Pascoal AM. Output synchronization of heterogeneous LTI plants with event-triggered communication. *Proc. of the 53rd Conf. on Decision and Control*, Los Angeles, CA, USA, 2014; 3572–3577, doi:10.1109/CDC.2014.7039944.
35. Tallapragada P, Chopra N. Event-triggered dynamic output feedback control for LTI systems. *Proc. of the 51st Conf. on Decision and Control*, Maui, Hawaii, USA, 2012; 6597–6602, doi:10.1109/CDC.2012.6426217.
36. Moreau L. Stability of continuous-time distributed consensus algorithms. *Proc. of the 43rd Conf. on Decision and Control*, Atlantis, Paradise Island, Bahamas, 2004; 3998–4003, doi:10.1109/CDC.2004.1429377.
37. Mazo Jr M, Tabuada P. Decentralized event-triggered control over wireless sensor/actuator networks. *IEEE Transactions on Automatic Control* Oct 2011; **56**(10):2456–2461, doi:10.1109/TAC.2011.2164036.
38. Tallapragada P, Chopra N. Event-triggered decentralized dynamic output feedback control for LTI systems. *Proc. of the 3rd IFAC Workshop on Distributed Estimation and Control in Networked Systems*, Santa Barbara, CA, USA, 2012; 31–36, doi:10.3182/20120914-2-US-4030.00057.
39. Mazo Jr M, Cao M. Decentralized event-triggered control with asynchronous updates. *Proc. of the 50th Conf. on Decision and Control and 2011 European Control Conf.*, Orlando, FL, USA, 2011; 2547–2552, doi:10.1109/CDC.2011.6160582.
40. Arzén KE. A simple event-based PID controller. *Preprints of the 14th IFAC World Congress*, Beijing, P.R. China, 1999; 423–428.
41. Lehmann D, Lunze J. Event-based output-feedback control. *19th Mediterranean Conf. on Control and Automation*, Corfu, Greece, 2011; 982–987, doi:10.1109/MED.2011.5983002.
42. Shi P, Wang H, Lim CC. Network-based event-triggered control for singular systems with quantizations. *IEEE Transactions on Industrial Electronics* Feb 2016; **63**(2):1230–1238, doi:10.1109/TIE.2015.2475515.
43. Godsil C, Royle G. *Algebraic Graph Theory*. Graduate Texts in Mathematics, Springer-Verlag: New York, USA, 2001.
44. Ren W, Beard RW, Atkins EM. Information consensus in multivehicle cooperative control. *IEEE Control Systems Magazine* Apr 2007; **27**(2):71–82, doi:10.1109/MCS.2007.338264.
45. Lin Z, Francis B, Maggiore M. Necessary and sufficient conditions for formation control of unicycles. *IEEE Transactions on Automatic Control* Jan 2005; **50**(1):121–127, doi:10.1109/TAC.2004.841121.
46. Haddad WM, Chellaboina V, Nersisov SG. *Impulsive and Hybrid Dynamical Systems*. Princeton Univ. Press: Princeton, NJ, USA, 2006.
47. Goebel R, Sanfelice RG, Teel AR. Hybrid dynamical systems. *IEEE Control Systems Magazine* Apr 2009; **29**(2):28–93, doi:10.1109/MCS.2008.931718.
48. Khalil HK. *Nonlinear Systems*. 3rd edn., Prentice Hall: Upper Saddle River, New Jersey, USA, 2002.
49. Sontag ED, Wang Y. New characterizations of input-to-state stability. *IEEE Transactions on Automatic Control* Sep 1996; **41**(9):1283–1294, doi:10.1109/9.536498.
50. Boyd S, Vandenberghe L. *Convex Optimization*. Cambridge University Press, 2004.